Thesis for the degree of Licentiate of Engineering

Mathematical modelling of operating cycles for road vehicles

Luigi Romano

Department of Mechanics and Maritime Sciences
CHALMERS UNIVERSITY OF TECHNOLOGY
Göteborg, Sweden 2021

Mathematical modelling of operating cycles for road vehicles
Luigi Romano

Licentiatavhandlingar vid Chalmers tekniska högskola
Technical report No. 2021:09

Department of Mechanics and Maritime Sciences
Chalmers University of Technology
SE–412 96 Göteborg, Sweden
Telephone + 46 (0) 31 – 772 1000

Typeset by the author using LaTeX.

Printed by Chalmers Reproservice
Göteborg, Sweden 2021

I like boring things

– Andy Wharol

Abstract

Difficulties that commercial vehicles are facing in meeting regulation standards require *ad-hoc* solutions. Emissions can be dramatically lowered if the characteristics of the transport application are known in advance. To tailor the vehicle's specification towards the use-case, however, a representative description of the mission, together with the surroundings, is needed.

Where many conventional approaches fail, the operating cycle format (OC) has shown promising results in describing road operations in a way which is completely independent of both vehicle and driver. More specifically, the framework consists of three levels of representation. The first, called the *bird's eye view*, serves mainly as a classification tool, and makes use of metrics and labels to completely characterise the overall application of a vehicle during its lifetime. The second description, the *stochastic operating cycle* (sOC), condenses the main properties of a road operation using elementary statistics. It is conceived as an intermediate representation with a higher degree of accuracy. Finally, the *deterministic operating cycle* (dOC) is the most detailed description of a transport mission, and collects deterministic models to be used in simulation.

In previous studies, the OC format was demonstrated to work in theory, but some margins for improvement could still be identified. Furthermore, the utility and benefits deriving from the use of the OC in concrete situations was explored only partially.

The main objective of this thesis consists in extending the OC representation to include stochastic models for weather and traffic, which were missing in the original formulation. The new models are built to be parsimonious and to allow ease of parametrisation and implementation starting from real data. This enables to reproduce and simulate realistic environments where a transport mission can take place, with a substantial gain in accuracy.

The second purpose of this work is to showcase how the OC concept can be used in practical applications involving real customers. A case study is presented to exemplify the advantages connected with the use of the OC description in product selection, prospecting a potential reduction of fuel consumption and emission of about 10%.

Keywords: operating cycle, transport application, road mission, stochastic models, autoregressive models, energy estimation.

Acknowledgments

There are many people which contributed more or less directly to this achievement.

First of all, I would like to express my gratitude to Dr. Fredrik Bruzelius, Dr. Sixten Berglund and Prof. Bengt Jacobson for offering me the amazing opportunity of embarking on a PhD journey. As main supervisor, Fredrik also deserves special thanks for the exceptional guidance provided during the last two years. His academic background and different perspective on many theoretical problems were a continuous source of inspiration. Fredrik, thank you also for supporting my own ideas and letting me explore them in total freedom. Bengt, you have the same curious spirit of a child. Your comments are always enlightening, and often spurred me to approaching problems from another angle. Sometimes it is hard to swim among your thoughts, but I have learned that it is always worth it. I thank you for that. To Sixten goes my sincere gratitude for the nice time spent together in Lundby, especially during the running sessions, and for the supervision provided during the first part of my PhD.

From Volvo side, I would like to thank Rickard Andersson and Anders Eriksson for their support and their involvement in the project. A special mention goes to Pär Johannesson at RISE, who introduced me to the intriguing world of statistics, and Pär Pettersson, who preceded me in COVER: without your fundamental contribution, most of the work in this thesis would have never been possible. To some extent, I am in debt with you. Finally, I would like to thank my brilliant student Erik Nordström for his great contribution to the project. It was a pleasure to meet and supervise you, even from remote.

At Chalmers, I am particularly thankful to Simone and Sonja for taking care of all the administrative stuff. Sonja is always there to help with a warm smile, and incarnates the spirit of VEAS in the most gentle way. Simone, thank you for letting me spend some time abroad with my family, I really appreciated that. In Napoli, I also had the opportunity to collaborate again with Prof. Francesco Timpone, to whom I express, as always, my sincere affection. He has the special merit of firstly introducing me to the fascinating discipline of vehicle dynamics.

My colleagues at Chalmers always create an enjoyable work environment: thank you for that, especially for many hilarious moments during Friday's fika. With Dragan I had many interesting conversations about love, poetry, philosophy and Murakami's books. I hope we can share soon some thoughts over a cold beer. Toheed and I are united by a sincere passion for sci-fi movies. I would spend hour talking about that. Tushar, you know how to consume my time engaging me in pleasant 'nerdy' discussion. It is always nice to grab a cup of coffee together.

During these two years I also had the chance of spending time with many people outside VEAS. I particularly enjoyed my time with Carl-Johan and Sondre from the control group.

Thank you for the interesting discussions and for all our pre-lecture coffees. In Michele Maglio I recently find a nice lunch mate. I hope we can deepen our friendship even more in the time to come.

Outside Chalmers, I would like to to thank my great friends Ali and Afshin, and all the Kantareller guys from our crazy Italian community: Milo, Antonio, Giovanni, Erik, Matteo, Matteo Tamini, Anton and Sergio. Milo, I am especially grateful to you for welcoming me in Sweden since the very beginning, and for our long and interesting discussions about maths and PDEs.

Lastly, I would like to thank my family. Mom, dad, and Checco, thank you for supporting me from Italy and believing in me. I love you immensely.

Yulia, my beloved *piccerella*, you have always been my precious light. I treasured every single moment with (and even without) you.

Göteborg, May 2021

List of Publications

This thesis is based on the following appended papers:

Paper 1. Luigi Romano, Erik Nordström, Fredrik Bruzelius, Rickard Andersson and Bengt Jacobson. *A case study of usage modelling of heavy vehicles using the operating cycle description.* Submitted (2021).

Paper 2. Luigi Romano, Pär Johannesson, Fredrik Bruzelius and Bengt Jacobson. *An enhanced stochastic operating cycle description including weather and traffic models.* Accepted for publication by Transportation Research Part D: Transport and Environment.

Paper 3. Luigi Romano, Francesco Timpone, Fredrik Bruzelius and Bengt Jacobson. *A theoretical investigation on transient tyre slip losses using the brush theory.* Submitted (2021).

In both Papers 1 and 3, the author was the major responsible for conceptualisation, modelling, analytical investigation, simulation and writing. The other authors contributed with valuable discussions, supervision and reading the manuscript. Paper 2 is mostly based on the master's thesis by Nordström (2020), whom the author supervised. The manuscript was written by the author.

Other relevant publications not included in this thesis:

Luigi Romano, Francesco Timpone, Fredrik Bruzelius, Bengt Jacobson. *Analytical results in transient brush models.* Submitted (2021).

Luigi Romano, Fredrik Bruzelius, Bengt Jacobson. *A Brush Tyre Model with Standstill Handler for Energy Efficiency Studies.* In: Berns K., Dressler K., Kalmar R., Stephan N., Teutsch R., Thul M. (eds) Commercial Vehicle Technology 2020/2021. Proceedings, pp. 119-134. 2021.

Luigi Romano, Fredrik Bruzelius, Bengt Jacobson. *Unsteady-state brush theory.* Vehicle System Dynamics. Vol. In Press. 2020.

Luigi Romano, Fredrik Bruzelius, Bengt Jacobson. *Brush tyre models for large camber angles and steering speeds.* Vehicle System Dynamics. Vol. In Press. 2020.

Luigi Romano, Salvatore Strano, Mario Terzo. *Synthesis and comparative analysis of three model-based observers for normal load and friction estimation in intelligent tyre concepts.* Proceedings of the Institution of Mechanical Engineers, Part D: Journal of Automobile Engineering. Vol. In Press, pp. 1-14. 2020.

Luigi Romano, Aleksandr Sakhnevych, Salvatore Strano, Francesco Timpone. *A novel brush-model with flexible carcass for transient interactions.* Meccanica. Vol. 54 (10), pp. 415-420. 2019.

Giovanni Breglio, Andrea Irace, Vincenzo Romano Marrazzo, Michele Riccio, **Luigi Romano**, Salvatore Strano, Mario Terzo. *Feel-tire Unina: Development and Modeling of a Sensing System for Intelligent Tires.* 2019 IEEE 5th International forum on Research and Technology for Society and Industry (RTSI), pp. 453-458. 2019.

Luigi Romano, Aleksandr Sakhnevych, Salvatore Strano, Francesco Timpone. *A hybrid tyre model for in-plane dynamics.* Vehicle System Dynamics. Vol. 58 (7), pp. 1123-1145. 2019.

Luigi Romano, Salvatore Strano, Mario Terzo. *A Model-Based Observer for Intelligent Tire Concepts.* 2019 IEEE 5th International forum on Research and Technology for Society and Industry (RTSI), pp. 447-452. 2019.

Daniel Garcia-Pozuelo, Oluremi Olatunbosun, **Luigi Romano**, Salvatore Strano, Mario Terzo, Ari J. Tuononen, Yi Xiong. *Development and experimental validation of a real-time analytical model for different intelligent tyre concepts.* Vehicle System Dynamics. Vol. 57 (12), pp. 1970-1988. 2019.

List of Acronyms

OC	–	Operating cycle
dOC	–	Deterministic operating cycle
sOC	–	Stochastic operating cycle

Contents

Part I

Introductory chapters

Chapter 1

Introduction

Fundamental research does not necessitate to be relevant from a practical perspective. It can be agreed, in fact, that it only needs to be sufficiently intriguing for someone to be done. However, the content of this thesis – which marginally touches upon some topics in vehicle dynamics – cannot be counted as fundamental research. Therefore, it is extremely important to place it into the right context.

1.1 Motivation and background

An appealing way to frame this thesis is to invoke some recently published data which demonstrate with striking evidence the prevalent anthropogenic contribution to the greenhouse effect. To cite a few documents, one can look at the technical reports authored by Callery (2019), Cook et al. (2013), Hausfather (2020), and Tol (2014), and those drafted by the C. C. C. Service (2019), European Environmental Agency (2019), Eurostat (2019), G. C. Project (2017), U. S. E. P. Agency (2019), and Union of concerned scientists (2019). A conspicuous contribution comes from the release of equivalent CO_2 emissions from human activity and, in particular relating to the transportation sector. This incentivised the European Commission (2014a,b, 2017, 2019) to adopt several strict measures contrasting the alarming trend of increasing temperature and pollution. More specifically, emission thresholds have been set for heavy-duty and passenger vehicles. Preliminary tests are aimed at ensuring compliance with these limits, and can be carried out physically or by using simulation tools. In this context, emissions can be significantly lowered if the vehicle's operating conditions are known in advance. Indeed, performance can be significantly enhanced depending on the mission characteristics, driver's behaviour, and external settings[1]. All these factors correlate with both the usage itself and the surrounding in which the transport operation takes place. Since major variation may occur depending on the location and the time[2], the vehicle's specifications should be tailored to meet not only the transport application, but also the relative boundary conditions. To investigate how these influence the vehicle's response, however, it is necessary to formulate mathematical models. These should of course be realistic, and ideally sufficiently simple to allow a

[1] Just to mention a few: topography, wind and traffic conditions *in primis*.

[2] We can refer at *first instance* to the effect exerted by seasonal trends.

fundamental understanding of the problem. Limiting the attention to the vehicle and driver as separate entities, several models have been developed over the years with different goals in mind. On the other hand, a synthetic but complete description of a transport operation has been rarely attempted in literature. One obvious difficulty encountered when defining a transport operation relates to the notion *per se*, which might appear to be rather obscure and vague. Provided that this first obstacle can be overcome, another question to address is how to identify all the relevant features, and then represent them in a useful manner, and in a way such they are independent of the vehicle itself. We will refer to this as the *representation problem*.

Accurate modelling of transport operations may also serve different purposes than the ones outlined so far. For heavy-duty vehicles, an important aspect to consider is that virtual testing is often required before a physical prototype can be built. One reason for that relates to the immense degree of diversification that can be achieved in the actual configuration. Indeed, whilst only few predetermined alternatives are available for passenger cars, the panorama of different combinations is virtually infinite for trucks. Considering the combinatorial nature of the problem, it becomes soon obvious that physical testing is prohibitive in terms of both costs and times, and other options should be preferred.

Tailoring the vehicle for the right mission – or spectra of missions – is an extremely delicate process. Besides, if all the relevant factors are not accounted properly, a solution derived analytically, or even numerically, can easily result in a suboptimal configuration in practice.

A preliminary answer to the representation problem has been formulated by Pettersson (2019) and formalised in the so-called *operating cycle* (OC) format. This type of description tries to capture the essential of the transport mission and the environment in a way which is completely independent of both the vehicle's and driver's characteristics. Therefore, unlike other common approaches, the OC framework enables a direct comparison between different vehicle configurations. Indeed, any contamination in the representation originating from the intrinsic dynamics of the vehicle is automatically avoided. In previous studies, the OC format has been demonstrated to be capable of reproducing a transport operation accurately and in a realistic way. At present, the implementation delivered by Pettersson, Johannesson, et al. (2019) is promising, and outperforms conventional descriptions. Nonetheless, it still has margins of improvements. Furthermore, the application of the OC framework has been manly limited to a theoretical domain. The scope of this thesis is hence to extend the OC format to incorporate new features, including weather and traffic, and to demonstrate how it can be used in practice. The research output is similar to an extended collection of formal tools which can be used to describe mathematically a transport operation, test virtual prototypes and algorithms, and make statistical inference.

1.1.1 Previous works

The aspects outlined so far are themselves sufficient to legitimate the enormous research effort lavished on addressing the representation problem. One well established approach consists of describing a transport mission using a driving cycle. Intuitively, a driving cycle is a map from the vehicle's position along its trajectory to a speed profile, which should capture the salient features of the operation. For an interested reader, a more

formal definition in mathematical terms can be found in Silvas (2015). In this context, speed profiles can be synthesised by using different types of information, and several approaches have been proposed in literature. In particular, there exist two main variants of a driving cycle: modal and transient. The former type is usually employed to for standard tests regulated by legislation, as in VECTO (Fontaras et al. 2013), since it allows for straightforward comparison. However, such driving cycles are not very realistic, and are becoming rapidly obsolete. Indeed, the main shortcoming of using them resides in the fact that performance is inherently built into the model, and there is no clear separation between the vehicle and driving cycle itself.

Transient cycles are often preferred for powertrain optimisation and design purposes, which require accurate feasibility studies, as the one performed by Åsbogåard et al. (2007), Basso, Kulcsár, Egardt, et al. (2019), Basso, Kulcsár, and Sanchez-Diaz (2021), Ghandriz (2018), Ghandriz, Hellgren, et al. (2016), and Ghandriz, Jacobson, Laine, et al. (2020). In this context, a crucial aspect for efficient design is the accurate description of a transport operation, with exhaustive information about the surroundings. Indeed, to correctly replicate real-world performance, it is necessary to take into account all the external factors and stimuli which may affect the vehicle's behaviour. These include road and mission properties, but also weather and traffic conditions (Llopis-Castelló et al. 2018; Sciarretta 2020; Sentoff et al. 2015; Wyatt et al. 2014).

How to synthesise representative transient cycles is an interesting and open question, and different approaches have been explored over the years. In particular, it is possible to distinguish between rule-based methods and statistical ones. Rule-based methods are very sensitive to experts' opinion and aim to replicate a limited number of characteristics from the measured driving cycles (Naghizadeh 2003; Zou et al. 2004). Such a criterion may be represented by the percentages of city, suburb, and highway speeds. By contrast, the advantage of resorting to statistical techniques resides in the fact that generated synthetic speed profiles correlate with certain operating conditions of the vehicle, e.g. cruising, idling, acceleration or braking events. This enhanced approach makes use of Markov chains or machine learning techniques, and combines different information (mostly inferred by speed and acceleration signals) to reflect the characteristics of real-driving scenarios. Improved algorithms also account for external sources of excitation (for example road grade) which are anticipated to have a major influence on a vehicle's overall performance (Amirjamshidi and Roorda 2015; Ashatari et al. 2014; Brady and O'Mahony 2016; Kamble et al. 2009; T. K. Lee and Filipi 2011; T. Lee et al. 2011; Lin and Niemeier 2002; Nyberg 2015; Silvas 2015; Silvas et al. 2016; Tazelaar et al. 2009). Traffic conditions are also modelled empirically, often based also on the characteristics of a certain road type (Sciarretta 2020).

1.1.2 The operating cycle representation

At this point, there are two main arguments which may be raised against these conventional driving cycles. The first is that their pathological nature makes them inadequate to compare different vehicles. With "pathological", we mean that there exists an implicit correlation between the reference vehicle and the speed profile. This intrinsic contamination may jeopardise the general validity of the resulting speed profile. Another demerit point is that, when a driving cycle is recorded, all the external effects (due to e.g. traffic or wind

conditions) are automatically incorporated. This is done implicitly, meaning that their influence cannot be understood or examined. Intuitively, we shall then argue that a general, reliable representation should be independent of both the vehicle and the driver.

The operating OC introduced by Pettersson (2019), Pettersson, Berglund, et al. (2019), and Pettersson, Johannesson, et al. (2019) certainly fulfills these requirements. In fact, this type of representation is not based on the concept of driving cycle, and therefore no speed profile needs to be prescribed as an input to the longitudinal vehicle mode. On the contrary, the properties of both the mission and the external surroundings are modelled separately, and then a driver model is used to translate dynamically the external stimuli into a desired speed. This allows to circumvent the need to incorporate the information coming from the surroundings into the speed profile.

The OC consists of three main levels of representation, each of them designed to a specific role. Before commenting on their relative function, we shall clarify the notions of *transport application*, *transport operation* and *transport mission* according to Pettersson (2019). In particular, Pettersson (ibid.) defines the transport application as the overall purpose of a vehicle during its lifetime. This is something antecedent to the vehicle itself, and towards which the specifications should be tailored. The difference between transport operation and mission is less formal: the former consists of a finite number of tasks along a given route, the latter integrates the operation with details from the surroundings. Both the operation and the mission presume the existence of a vehicle to make sense, i.e. are defined *a posteriori*.

Given the definitions above, our intuition suggests that having a realistic description of a transport mission is not sufficient to characterise the application. There are two additional requirements which we shall impose. The first one relates to existence of different sorts of relationships between individual representations. In nature, things can be grouped and labelled into different categories depending on certain common properties. Identifying differences and similarities between transport missions is crucial when it comes to defining the overall application. If transport missions can be classified based on some well-defined metrics, then the complexity of the problem decreases significantly. This need for a classification system is referred to as the *classification problem*. The second aspect connects to the *variation problem*. Indeed, provided that we are able to identify suitable metrics, even missions which belong to the same transport application cannot be expected to be identical when interpreted as individual realisations. Ideally, we would like to quantify the variation inside each category in a simple way. This implies, however, the need for an intermediate description, which should be ideally built around this principle and make use of elementary statistical tools.

The three levels of representation introduced by Pettersson (ibid.), namely the *bird's eye view*, the *stochastic operating cycle* (sOC) and the *deterministic operating cycle* (dOC), respond exactly to these needs.

Descending the hierarchical ordering existing between the descriptions, the bird's eye view collocates on the top of the pyramid. It is the answer suggested by Pettersson (ibid.) to address the classification problem. It characterises the entire application, and makes use of simplified metrics and labels. At the mid-level, the sOC summarises the statistical properties of a transport mission, and consists of a collection of stochastic models and parameters. It is conceived as a tool to investigate the variation problem. Finally, the

dOC is the representation with the highest level of detail, and is the envisioned solution to the representation problem.

In the sOC and dOC descriptions, every physical quantity may be described using statistical or deterministic models, respectively.

1.2 Research objectives

Two main research objectives can be identified for the present thesis.

The first deals with the pure representation problem, as defined by Pettersson (ibid.), and relates to the features to be included when describing a transport operation. Some of these – like wind and traffic conditions – were already indicated in Pettersson (2019), Pettersson, Berglund, et al. (2019), and Pettersson, Johannesson, et al. (2019) and anticipated to have a major impact upon energy efficiency. However, their influence was deliberately omitted for the sake of convenience. A major goal of this thesis is therefore to extend the OC representation initiated by Pettersson, Johannesson, et al. (2019) to include stochastic weather and traffic parameters. The approach is similar to the one proposed in Pettersson, Johannesson, et al. (ibid.), with every model being independent of the others. This allows to construct a modular framework in which virtual prototypes can be tested and different configurations evaluated.

The second research objective is to explore more deeply the relationship between the different levels of representation. The conceptual connection established by Pettersson was certainly consistent in theory, but its usefulness needs to be confirmed by some concrete application. An attempt to partially address this issue is made in Paper 1, in which it has been demonstrated how the three-level OC description can be used in practice when dealing with a customer.

1.3 Scientific contributions

The main scientific contributions of this thesis are:

- A first case study on the modelling of energy usage for heavy-duty vehicles using the operating cycle format. This has been the main object of Paper 1, where real log data have been used to parametrise the stochastic models for the road and mission categories.

- In Paper 2, an enhanced version of the sOC has been proposed which includes new stochastic models for the weather and traffic categories. It must be remarked that the stochastic models for weather and traffic do not constitute a novelty when considered in isolation, since a great deal of research has been already lavished on dedicated studies. Instead, the main contribution of the present work should be sought in that it makes this collection of stochastic models useful for studies in vehicle dynamics.

- A sensitivity study of the influence from seasonal and traffic settings upon the CO_2 emissions of a heavy-duty truck (Paper 2).

- Based on the general brush theory developed by Romano et al. (2020a,b), an improved understanding of the transient dissipation mechanisms connected with tyre slip losses (Paper 3).

- A new version of the open source platform VehProp, a simulation environment developed for studies of longitudinal vehicle dynamics. The current implementation includes novel models for weather and traffic, and a driver which reacts dynamically to the traffic density.

1.4 Theory and methods

With a little bit of intuition, one can realise that this is not a conventional thesis in vehicle dynamics. Quite the opposite, the focus is more on what surrounds the vehicle. More specifically, in the sOC description, the modelling of the operational environment is mainly based on stochastic processes. These, together with other elementary tools borrowed from the disciplines of probability and statistics, constitute the true core of the present research. In the main part of the thesis, we will however prefer a rather friendly approach to the topic, with emphasis on the physical aspects. A more rigorous introduction to the stochastic processes used in the building of the sOC format is given in Appendix A.

Conventional models for (longitudinal) vehicle dynamics are mainly based on systems of *differential-algebraic equations* (DAE). The reader is presumed to be familiar with the topic, which is not covered explicitly in the thesis. On the other hand, the results advocated in Paper 3 are based on the classic theory for linear PDEs, for which there exists a boundless amount of literature. Two useful references are the almost all-embracing book by Evans (2010) and the more gentle introduction by Ockendon et al. (2003). The findings of Paper 3 will be only briefly mentioned throughout the thesis, and hence no appendix is dedicated to the topic.

1.5 Limitations

Being the scope of the present research extremely broad, some assumptions have been introduced to simplify the analysis. This has inevitably led to some limitations.

In particular, from a pure vehicle modelling perspective, the analysis has been confined to longitudinal dynamics. The effect from suspension compliance has also been neglected systematically. The influence from tyre slip losses has been investigated mainly theoretically in Paper 3 and also numerically in Romano et al. (2021), but has been disregarded otherwise. In Paper 3 it was also shown that considering the transient behaviour of the tyre during acceleration and deceleration phases may lead to different results than the ones advocated in other studies, but, to the best of the author's knowledge, a proper model to account for the non-steady state slip losses has not been developed yet.

Some limitations are strictly connected to the stochastic models introduced in the operating cycle description. In particular, the physical quantities labelled in the road and weather categories have been assumed to only depend either on the space or time, respectively. Furthermore, the proposed traffic model is based on the assumption of

stationary flow and homogeneous road conditions, as discussed extensively in Sec. 2.3.4 and in Paper 2. Weather and traffic models have been built in isolation and parametrised using real data available from external databases. For both, the fitting procedures have been chosen such as to minimise the error between the model prediction and measurements. However, no experimental validation has been conducted with respect to signals available from log-data, mainly due to lack of information.

The examples used throughout the thesis deal with heavy-duty trucks equipped with diesel engines. However, the OC format has been conceived to be generally applicable to any (road) vehicle category, provided that a suitable model is available. Lastly, the driver model employed in this thesis is based on a simple PID controller and tries to replicate a human driver. Simulation results seem to suggest a realistic behaviour, but no experimental validation has been conducted.

1.6 Outline

The rest of this thesis is structured as follows: Chap. 2 is dedicated to the description of the OC format, and covers all the three levels of representation. A preliminary analysis is attempted do deduce mathematically which quantities to include when modelling the environment. The core of the chapter focusses on the novel features introduced in the sOC. In Chap. 3, the practical usage of the OC format is exemplified starting from the investigation conducted in Paper 1. The discussion is integrated with additional comments on some technical aspects which concern the parametrisation and the implementation of the stochastic models added in the thesis. Chapter 4 concludes the thesis summarising what done, and opening possible perspectives for future studies. The tone of the discussion is deliberately kept informal in the main chapters, but an introduction on the statistical tools used to build of the sOC can be found in Appendices A and B.

Chapter 2

The operating cycle description

This chapter is dedicated to the mathematical description of a road transport mission in terms of an operating cycle. We will try to understand which physical quantities affect the behaviour of a road vehicle, and how to model them in a way which is useful for the representation. The aim of the operating cycle is threefold, and should satisfy the needs for classification, variation and simulation. In this chapter, the focus is mainly on energy efficiency, but the results drawn in the subsequent paragraphs hold very generally. We shall start from an elementary set of equations for longitudinal vehicle dynamics, from which the most salient features to be included in such a description may be deduced. The idea is to consider in isolation the contribution of each physical quantity to the instantaneous power demand required to the propulsion, and hence, by straightforward integration, to the total energy. The analysis proposed in this chapter follows the one reported in Pettersson (2019) and Pettersson, Johannesson, et al. (2019), with few slightly more involving steps.

Once all the relevant factors have been identified, it is crucial to formulate adequate models to account for them. As already seen, this is a nontrivial task, which many conventional approaches have only partially succeeded in accomplishing. The operational cycle description proposed by Pettersson (2019) tries to overcome the issues encountered so far by introducing a dynamic description of the transport mission which is independent of the vehicle. Therefore, in the second part of the chapter, we will introduce in detail the three levels of representation upon which the complete operating cycle is built: the *bird's eye view*, the *stochastic operating cycle* (sOC) and the *deterministic operating cycle* (dOC). These three descriptions complement each other and attempt to address the classification, variation and simulation problems, respectively. In what follows, we will review them in order, with particular emphasis on the sOC, whose new features constitute the core of the present work. All the models presented in this chapter may be found in similar form in Pettersson (2019) and Pettersson, Johannesson, et al. (2019) and in Paper 2.

2.1 Longitudinal dynamics and energy consumption

To understand which factors must be included when dealing with energy efficiency studies, it is necessary to formalise the problem mathematically. To limit the scope of the present analysis, we will only deal with the longitudinal problem, i.e. neglect the lateral dynamics and vertical energy dissipation.

For a rigid truck[1], the complete set of equations governing the system dynamics may be easily inferred starting from Newton's Second Law as follows:

$$0 = -m\dot{v}_x + \sum_{i=1}^{n} F_{ix} - F_{\text{grade}} - F_{\text{air}}, \tag{2.1a}$$

$$0 = \sum_{i=1}^{n} F_{iz} - mg\cos\alpha, \tag{2.1b}$$

$$0 = \sum_{i=n_{\text{f}}+1}^{n} l_i F_{iz} - \sum_{i=1}^{n_{\text{f}}} l_i F_{iz} - h_G \sum_{i=1}^{n} F_{ix} - (h_{\text{air}} - h_G)F_{\text{air}}, \tag{2.1c}$$

$$0 = T_{\text{w}i} - R_{\delta i} F_{ix} - f_{\text{r}} R_{\delta i} F_{iz} - J_{\text{w}i}\dot{\omega}_{\text{w}i}. \tag{2.1d}$$

The above Eqs. (2.1a), (2.1b) and (2.1c) are the equations governing the longitudinal, vertical and rotational equilibrium for the entire vehicle in the (O, x, z) plane, whilst (2.1d) prescribes the rotational equilibrium of the i_{th} wheel, $i = 1, \dots, n$. The axles have been numbered from $i = 1, \dots, n$, starting from the first one at the extreme right. The number of axles located to the right of the centre of gravity (CoG) is n_{f}, whilst the axles behind the CoG are n_{r}. The total number of axles is given by $n = n_{\text{f}} + n_{\text{r}}$. In Eq. (2.1a), we have denoted by F_{ix} the longitudinal forces exerted at the tyre-road interface, by F_{grade} the longitudinal component of the gravitational force, and by F_{air} the air resistance. The terms h_{air} and h_G appearing in Eq. (2.1c) represent the height of the air resistance and centre of gravity with respect to the road, or, more precisely, to the contact points of the tyres; l_i is the longitudinal distance of the i_{th} axle from the centre of gravity G. Finally, in Eq. (2.1d), $T_{\text{w}i}$ is the total torque applied to the wheel i, $J_{\text{w}i}$ its rotational inertia, and $R_{\delta i} \triangleq R_{\text{w}i} - \delta_i$ the deformed radius of the tyre, where $R_{\text{w}i}$ is the nominal wheel radius and δ_i the maximum vertical deformation due to the normal load F_{iz}. The quantity f_{r}, here assumed constant for each tyre, represents the rolling resistance coefficient.

The generic torque acting on the wheel i may be separated into a component due to braking, namely $T_{\text{b}i}$, and another one coming from the prime mover $T_{\text{d}i}$, i.e. $T_{\text{w}i} = T_{\text{d}i} + T_{\text{b}i}$. By doing so, under the assumption of negligible internal losses, the power needed to move the vehicle may be computed as

$$P_{\text{d}} = \sum_{i=1}^{n} T_{\text{d}i}\omega_{\text{w}i} = v_x \sum_{i=1}^{n} \frac{T_{\text{d}i}}{R_{\text{r}i}\,(1 - \sigma_{ix})}, \tag{2.2}$$

where σ_{ix} is the *theoretical longitudinal slip*, defined as:

$$\sigma_{ix} \triangleq \frac{\omega_{\text{w}i} R_{\text{r}i} - v_x}{\omega_{\text{w}i} R_{\text{r}i}}, \tag{2.3}$$

and $R_{\text{r}i}$ is the so-called *rolling radius*. In general, it is greater than the deformed radius of the tyre and reads in first approximation $R_{\text{r}i} \simeq R_{\delta i} + 2\delta_i/3$ for small camber angles.

[1]For a rigid truck, we may fairly assume to have only one grade angle α. The set of equations for the case of an articulated vehicle is much more involving and derived in Ghandriz (2020) and Ghandriz, Jacobson, Nilsson, et al. (2020).

Combining Eqs. (2.1a), (2.1d), (2.2) and (2.3) yields, after some manipulations,

$$P_{\mathrm{d}} = v_x \left[\sum_{i=1}^{n} \frac{R_{\delta i} F_{ix} + f_{\mathrm{r}} R_{\delta i} F_{iz} + T_{\mathrm{b}i}}{R_{\mathrm{r}i}(1-\sigma_{ix})} + \frac{\sum_{i=1}^{n} F_{ix} - F_{\mathrm{grade}} - F_{\mathrm{air}}}{m} \sum_{i=1}^{n} \frac{J_{\mathrm{w}i}}{R_{\mathrm{r}i}^2 (1-\sigma_{ix})^2} \right] - v_x^2 \sum_{i=1}^{n} \frac{J_{\mathrm{w}i} \left[\dot{R}_{\mathrm{r}i}(1-\sigma_{ix}) - R_{\mathrm{r}i} \dot{\sigma}_{ix} \right]}{R_{\mathrm{r}i}^3 (1-\sigma_{ix})^3}. \tag{2.4}$$

The expression above is quite complicated, but may be simplified by introducing some additional assumptions. The main argumentation is that, in normal driving conditions, the last summation appearing in Eq. (2.4) is negligible when compared to the first two, and shall be disregarded henceforth. This simplifications approximately holds when sufficiently small changes in the slip occur[2] and the tyres work in the linear range of their normal characteristic. The latter conditions imply small vertical deformations δ_i and hence $R_{\delta i} \simeq R_{\mathrm{r}i} \equiv R_{\mathrm{w}i}$. Therefore, we may write:

$$P_{\mathrm{d}} \simeq v_x \left[\sum_{i=1}^{n} \frac{R_{\mathrm{w}i} F_{ix} + f_{\mathrm{r}} R_{\mathrm{w}i} F_{iz} + T_{\mathrm{b}i}}{R_{\mathrm{w}i}(1-\sigma_{ix})} + \frac{\sum_{i=1}^{n} F_{ix} - F_{\mathrm{grade}} - F_{\mathrm{air}}}{m} \sum_{i=1}^{n} \frac{J_{\mathrm{w}i}}{R_{\mathrm{w}i}^2 (1-\sigma_{ix})^2} \right]. \tag{2.5}$$

To analyse the expected amount of power to be delivered during an acceleration phase, we may comment on the remaining terms. Starting from the last one, the summation

$$\chi_m \triangleq \frac{1}{m} \sum_{i=1}^{n} \frac{J_{\mathrm{w}i}}{R_{\mathrm{w}i}^2 (1-\sigma_{ix})^2} > 0 \tag{2.6}$$

may be interpreted as an additional inertial term which adds to the real mass. It depends not only on the inertial and geometric parameters of the wheels, but also on the longitudinal slip variables σ_{ix}. These are, in normal driving conditions, usually smaller than a critical value. i.e. $|\sigma_{ix}| < \sigma_i^{\mathrm{cr}}(F_{iz}, \mu_i) < 1$. The critical slip $\sigma_i^{\mathrm{cr}}(F_{iz}, \mu_i)$ depends on many parameters, included the vertical load F_{iz} acting on each axle and the friction coefficient μ_i. The denominators in the first term are hence positive, and so are the quantities $f_{\mathrm{r}} R_{\mathrm{w}i} F_{iz}$ and $T_{\mathrm{b}i}$.

Under steady-state conditions, the longitudinal forces themselves are a function of the slip, and concordant with it, i.e.

$$F_{ix} = f_i(\sigma_{ix}, F_{iz}, \mu_i) = |f_i(\sigma_{ix}, F_{iz}, \mu_i)| \operatorname{sgn} \sigma_{ix}. \tag{2.7}$$

Owing to Eq. (2.7), it may be easily verified that

$$\sum_{i=1}^{n} \frac{F_{ix}}{1-\sigma_{ix}} \geq \sum_{i=1}^{n} F_{ix}, \tag{2.8}$$

[2] A situation where this condition is not fulfilled is, for example, acceleration from standstill in presence of nonzero road grade.

since the previous condition may be restated as

$$\sum_{i=1}^{n} \frac{F_{ix}\sigma_{ix}}{1-\sigma_{ix}} = \sum_{i=1}^{n} \frac{|f_i(\sigma_{ix}, F_{iz}, \mu_i)||\sigma_{ix}|}{1-\sigma_{ix}} \geq 0, \qquad 0 \leq \sigma_{ix} < \sigma_i^{\mathrm{cr}}, \tag{2.9}$$

or equivalently

$$\sum_{i=1}^{n} F_{ix}\kappa_i = \sum_{i=1}^{n} |f_i(\kappa_{ix}, F_{iz}, \mu_i)||\kappa_i| \geq 0, \qquad 0 \leq \kappa_i < \kappa_i^{\mathrm{cr}}, \tag{2.10}$$

where we have introduced the notion of practical slip[3] $\kappa_i = \sigma_{ix}/(1-\sigma_{ix})$, as defined in Pacejka (2012). It is worth noticing that, when multiplied by the longitudinal speed v_x, the practical slip κ_i returns the macro-sliding velocity of the tyre, and therefore the summations in Eqs. (2.9) and (2.10) actually represent the total slip losses in conditions close to steady-state[4]. These contribute partially to the overall energy dissipation (Beckers et al. 2019, 2020; Kobayashi, Katsuyama, Sugiura, Hattori, et al. 2020; Kobayashi, Katsuyama, Sugiura, Ono, et al. 2017, 2018; Torinsson et al. 2020), but are often erroneously neglected.

Taking into account (2.8) and assuming, for the sake of simplicity, $T_{\mathrm{b}i} = 0$, it is possible to deduce:

$$P_{\mathrm{d}} \geq v_x\Big(F_{\mathrm{grade}} + F_{\mathrm{air}} + F_{\mathrm{roll}} - F_{\mathrm{inertia}}\Big), \tag{2.11}$$

where the inertial term $F_{\mathrm{inertia}} = -m^*\dot{v}_x$ accounts for the effective mass $m^* = m(1+\chi_m)$ and the effective total rolling resistance $F_{\mathrm{roll}} \triangleq f_{\mathrm{r}} \sum_{i=1}^{n} F_{iz}/(1-\sigma_{ix})$ include the contribution due to the longitudinal slips[5]. The final expression to the right-hand side of Eq. (2.11) should be now very familiar, since it coincides formally with the classic one obtained for zero longitudinal slip, i.e. $\sigma_{ix} = 0$.

An additional amount of power may be required to supply the request from standard auxiliary devices, or from specific mission equipment. Denoting them by P_{aux} and P_{PTO}, the total power to be delivered by the prime mover is given by

$$P_{\mathrm{tot}} = P_{\mathrm{d}} + P_{\mathrm{aux}} + P_{\mathrm{PTO}}. \tag{2.12}$$

We continue now by commenting on each term showing in Eq. (2.11) separately. In particular, the following contributions can may identified:

- $F_{\mathrm{inertia}} = -m^*\dot{v}_x$. This term is proportional to the vehicle's acceleration and to the augmented mass $m^* = m + \chi_m$. Therefore, it includes implicitly any factor which may cause the vehicle to change its speed dynamically. Depending on the traffic and weather conditions, a driver may choose the desired speed based on the following quantities: traffic density, precipitation and asphalt properties. According to Eq. (2.6), the total inertial force is also influenced by the slip variables σ_{ix}, and therefore by the mechanical properties of the tyres.

[3] We have implicitly assumed that $\operatorname{sgn}\kappa_i = \operatorname{sgn}\sigma_{ix}$, which is always true for conventional driving scenarios.

[4] In transient conditions, the calculation of power slip losses based on a global equilibrium approach turns out to be fallacious, as discussed extensively in Romano et al. 2020a.

[5] In general, it is not obvious that $\sum_{i=1}^{n} F_{iz}/(1-\sigma_{ix}) \geq mg\cos\alpha$.

- $F_{\text{grade}} = -mg\sin\alpha$, where α is the road grade angle and the vehicle coordinate system defined according to ISO 8855. The slope angle is often described as a road gradient measured as a percentage. It is a road parameter and an exhaustive description may be found in Pettersson (2019) and Pettersson, Johannesson, et al. (2019).

- $F_{\text{roll}} = f_{\text{r}} \sum_{i=1}^{n} F_{iz}/(1-\sigma_{ix})$, in which f_{r} is the rolling resistance coefficient. The previous equation models empirically the energy loss due to viscoelastic properties of the tyre in its interaction with the road surface[6]. The road properties depend on the road properties, ground type and weather conditions. The longitudinal slips σ_{ix} also contribute to the rolling resistance.

- $F_{\text{air}} = \rho_{\text{air}} C_{\text{d}} A \left|v_x^{\text{rel}}\right| v_x^{\text{rel}}/2$, with ρ_{air} the air density, C_{d} the drag coefficient, A the effective frontal area and v_x^{rel} is the relative speed between the vehicle and the wind. The square dependence on the speed emphasises the need for the properties mentioned in the inertial term. Also, there are different physical quantities which are relevant to correctly take into account the contribution of the drag force. The first thing to be noticed is that the speed in question is the relative one between vehicle and wind; hence, a wind model is needed. Furthermore, the air density ρ_{air} is a function of the air pressure p_{air} and temperature T_{air}. The simplest model which accounts for this interaction is that of an ideal gas:

$$\rho_{\text{air}} = \frac{p_{\text{air}}}{RT_{\text{air}}}. \tag{2.13}$$

  Equation (2.13) justifies the necessity of detailed models for the air temperature and pressure. As a secondary effect, the external temperature might also influence a combustion engine's efficiency.

The terms identified above constitute a solid basis for a preliminary understanding of what should be included when representing a transport operation. It must be pointed out that there are several others factors to consider which do not appear explicitly in Eqs. (2.11) and (2.12). For example, the influence of side slip angle could be noteworthy to taken into account[7], but it requires more sophisticated in-plane models. Mechanical losses also take place in other components, e.g. suspensions and internal transmissions. The contribution from some external effects, due for example to traffic or weather conditions, may necessitate of an intermediate step to be interpreted and modelled properly, as discussed later. In the subsequent paragraphs, we will introduce the three level of description which constitute the complete OC representation.

2.2 The bird's eye view

The bird's eye view is the less detailed level of an operating cycle description. It is conceived to be very general, allowing for straightforward classification of transport applications

[6] For an exhaustive review of analytical tyre models, the reader is referred to the classic theories treated in Guiggiani (2018) and Pacejka (2012), or to the more recent works by Romano et al. (2020a,b).

[7] As also explained in Ghandriz (2020) and Ghandriz, Jacobson, Nilsson, et al. (2020).

based on few statistical indicators. These should be ideally chosen to be representative of some variation in usage, performance or properties.

At present, the formal description has only been sketched by Pettersson, Berglund, et al. (2019), and no scientific way of setting labels and metrics has been fully explored. A rigorous attempt to connect the bird's eye view to already-existing classification systems may be found in Pettersson, Johannesson, et al. (2019) and indirectly in Paper 1, where the GTA system (Edlund and Fryk 2004) is used as a starting point to proceed to mission classification. Later on, in Sect. 2.5, we will comment briefly on the connection between the three levels of representation making the OC.

As an example, for the topography parameter, the GTA system specifies four different levels:

1. `FLAT` if the slopes with gradient of less than 3% occur during more than 98% of the driving distance, and the maximum gradient is 8%.

2. `P-FLAT` if the slopes with gradient of less than 6% occur during more than 98% of the driving distance, and the maximum gradient is 16%.

3. `HILLY` if the slopes with gradient of less than 9% occur during more than 98% of the driving distance, and the maximum gradient is 20%.

4. `V-HILLY` if the other criteria are not fulfilled.

The thresholds set in the above list are however ambiguous, and there is no guarantee that they can reflect any significant variation in usage or performance.

One main advantage of such a vague description, on the other hand, resides in its colloquial tone. Indeed, the bird's eye view is the most appropriate description when interfacing the customer, which is not expected to have a deep understanding of stochastic models and parameters.

2.3 The stochastic operating cycle

The stochastic operating cycle (sOC) may be considered as a mid-level description of a transport mission. In its general formulation, it should ideally consist of a complete set of stochastic models grouped into four different categories: road, weather, traffic and mission. However, the current implementation only collects models for the first three categories.

Each sOC model is provided with its own set of stochastic parameters, which are chosen to condense the relevant statistical properties (mean, variance, ecc.) of the corresponding physical quantity. These may also be themselves related to physical entities, but the interpretation is often less straightforward. The structure of the sOC is conceived to be as simple as possible, and the models are thought to be independent of each other. In a more formal way, the complete set of sOC parameters may be defined mathematically as:

$$\mathcal{OC}_\mathrm{s} = \{\mathcal{R}_\mathrm{s}, \mathcal{W}_\mathrm{s}, \mathcal{T}_\mathrm{s}, \mathcal{M}_\mathrm{s}\}, \tag{2.14}$$

where $\mathcal{R}_\mathrm{s}$, $\mathcal{W}_\mathrm{s}$, $\mathcal{T}_\mathrm{s}$ and $\mathcal{W}_\mathrm{s}$ are the sets containing all the sOC parameters marked as road, weather, traffic and mission, respectively. Models and parameters for the road have

been introduced by Pettersson, Johannesson, et al. (2019), whilst the traffic and weather categories have been developed by the author in Paper 2 and constitute the novel features of the sOC.

We remark that the overall framework is built with the philosophy of being as simple as possible. This means that complicated multivariate distributions are avoided, thus requiring each individual model to be treated as a separate entity. Disregarding such mutual interaction guarantees modularity and allows for ease of implementation. At the same time, to balance complexity and realism, a certain level of interaction between each model is preserved by arranging the sOC itself in a hierarchical fashion. Parsimony is thus achieved by defining two separate set of models: primary and secondary ones (subordinate). In this way, it becomes possible to achieve a modular structure equipped with a high level of diversification. The (main) obvious disadvantage is that the number of effective values needed for each stochastic parameter also increases.

2.3.1 Primary models

Primary models are introduced to simplify the mathematical description of the format. At present, they include stochastic model for *road type* and *seasonality* falling within the road and weather categories, respectively.

The road type *per se* is an abstract notion, which cannot be measured or classified directly. The solution envisioned by Pettersson, Johannesson, et al. (ibid.) is hence to connect this concept to something which can be more easily understood and quantified: the speed limit (Ntziachristos and Samaras 2018). A stochastic model is then constructed by modelling the road type as piecewise constant function of the speed limit, which, in turn, is a piecewise constant function of the vehicle's position on the road. The resulting model is a marked Poisson process, as explained in detail in Sect. 2.3.2.

On the other hand, the model for seasonality is much simpler and only based on the stationary distribution for each season. In this context, it is worth noticing that, in the sOC, the seasons are regarded as meteorological ones.

Once a mathematical formulation for both primary models has been established, the secondary ones inherit their sets of sOC parameters accordingly. In particular, the sOC parameters for the secondary models in the road and weather categories are supposed to only depend on the corresponding primary counterpart. On the contrary, the stochastic parameters for the secondary traffic model are determined by the specific combination of road type and season. An illustration of the resulting composite edifice is shown in Fig. 2.1, where the hierarchical structure comprising primary and secondary models is shown.

In the following, the secondary models for the road, weather and traffic categories will be discussed in detail.

2.3.2 Secondary road models

The road parameters have been developed completely by Pettersson, Johannesson, et al. (2019), but are recalled here to give a complete overview of the sOC.

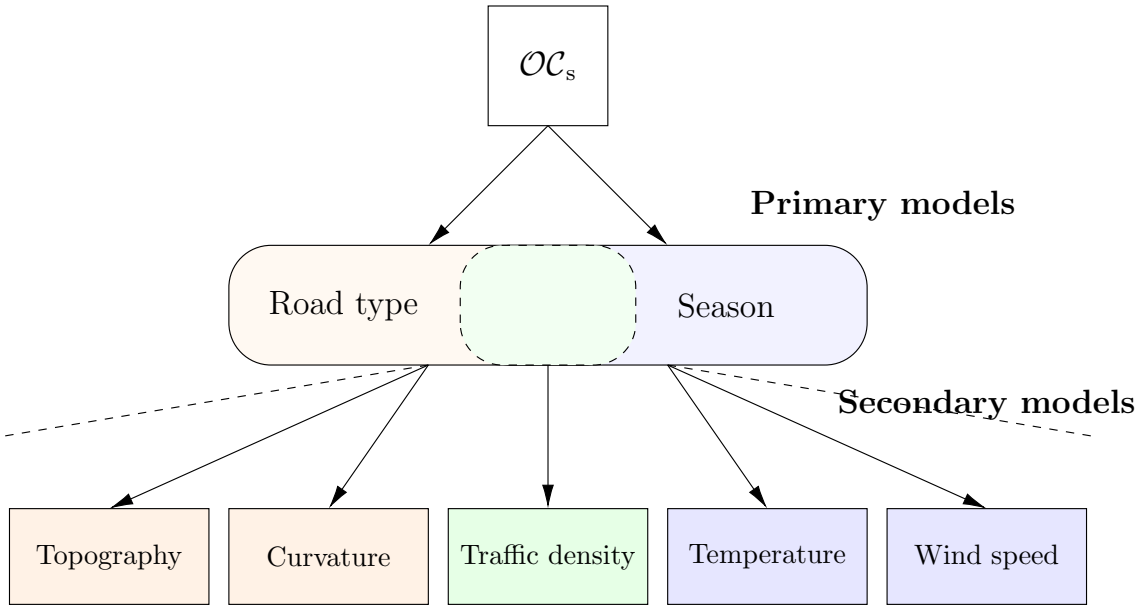

Figure 2.1: Hierarchical structure of an sOC. Road type and season are both primary models and influence the value of the statistical parameters for the secondary models. Whilst the (secondary) road and weather parameters depend only on the respective primary model, the traffic ones are determined by the road type and season simultaneously. Figure adapted from Paper 2.

Stop signs, give way signs, traffic lights and speed bumps

These entities are introduced simultaneously, since they behave in a similar way (Pettersson 2019; Pettersson, Johannesson, et al. 2019). They may be regarded as discrete entities and modelled in three parts: location, recommended speed and standstill time.

Starting from the sign locations, the collection of consecutive positions may be modelled as a sequence of random variables $\{X_k\}$ and treated as events scattered randomly between the start and end points. In this model, the road is partitioned into short segments, and thus the probability of occurrence of an event is only determined by the length of each segment. The simplest stochastic model with this property is the Poisson process (see Eq. (A.22) in Appendix A for further clarifications). The position of the events may be characterised by considering the difference between two consecutive occurrences:

$$X_{k+1} - X_k \sim \mathcal{E}(\lambda_s), \tag{2.15}$$

where $\mathcal{E}$ is the exponential distribution and λ_s is the intensity, interpreted as the mean number of events per unit of distance. Naturally, there is one intensity for each property.

At any given location k, the event has two additional properties: standstill time T_k and recommended speed V_k. For both the parameters, Pettersson, Johannesson, et al. (2019) propose to use a uniformly-distributed random number. In particular, the standstill time is allowed to range between a minimum $t_{\min}$ and maximum $t_{\max}$:

$$T_k \sim \mathcal{U}\big(t_{\min}, t_{\max}\big). \tag{2.16}$$

Similarly, the recommended speed is uniformly-distributed between a minimum $v_{\min}$ and maximum $v_{\max}$:

$$V_k \sim \mathcal{U}\Big(v_{\min}, v_{\max}\Big). \tag{2.17}$$

The five numeric values describing the intensity, standstill time bounds and recommended speed bounds fully describe the give way sign model. The stop sign model is fully parametrised by the intensity and standstill time bounds values.

Speed signs and ground type

These road properties behave as piecewise constant, right-side continuous functions of the position. Since the same stochastic model is used for both entities, we will only discuss the speed signs. These are treated as a random process $V = V(x)$ along the position $x \in \mathbb{R}$ on the road. The variable $V(x)$ is only allowed to take discrete values in the state space $\mathcal{S}_V = \{v_1, ..., v_{n_v}\}$, where n_v denotes the finite number of possible speed limits. The entire process is then split in two parts and modelled as a sequence of positions $\{X_k\}$, with the locations of the signs, and a sequence of speeds $\{V_k\}$.

It is also assumed that the current speed limit exerts the greater part of the influence on the upcoming limit. Therefore, we may approximate the probability of the speed limit occurrence as follows:

$$\mathbb{P}\Big(V_{k+1} = v_{i,k+1}\Big|V_1 = v_{i,1}, V_2 = v_{i,2}, \ldots, V_k = v_{i,k}\Big) \approx \mathbb{P}\Big(V_{k+1} = v_{i,k+1}\Big|V_k = v_{i,k}\Big). \tag{2.18}$$

The above Eq. (2.18) satisfies the Markov property A.2.1, and enables us to model the sequence as a Markov chain (the reader is referred to the Appendix A for a friendly introduction to the topic). Like the continuous process $V(x)$, the state space of $\{V_k\}$ refers to the possible speed limits already mentioned. Furthermore, since every new speed limit requires a sign to announce it, the model is embedded in that of the sign locations, so $k \in \mathbb{N}$.

The Markov probability matrix $\mathbf{P}_V \in \mathbb{R}^{n_v \times n_v}$ fully characterises such a chain. An entry p_{Vij} describes the probability of transitioning from state i to state j. This description may be reduced further by noticing that the speed limit model is embedded in that of the locations and there are no self-transitions, so all diagonal elements vanish, i.e. $p_{Vii} = 0$. The off-diagonal elements may then be described as the observed number of changes f_{Vij} between states i and j:

$$p_{Vij} = \frac{f_{Vij}}{\sum\limits_{j=1}^{n_v} f_{Vij}}. \tag{2.19}$$

The speed sign locations may be modelled as in Eq. (2.15). However, each state is expected to have its own intensity: n_v states introduces n_v intensities $\lambda_1, ..., \lambda_{n_v}$. Lastly, we introduce the mean length $L_{\mathrm{m}i}$ of speed limit v_i,

$$L_{\mathrm{m}i} = \frac{1}{\lambda_i}. \tag{2.20}$$

Thus, the complete description consists of the matrix f_{Vij} and the n_v mean lengths $L_{\mathrm{m}i}$.

The modelling of the road type follows automatically. It may be represented as a stochastic process starting from the speed limit (Ntziachristos and Samaras 2018). If

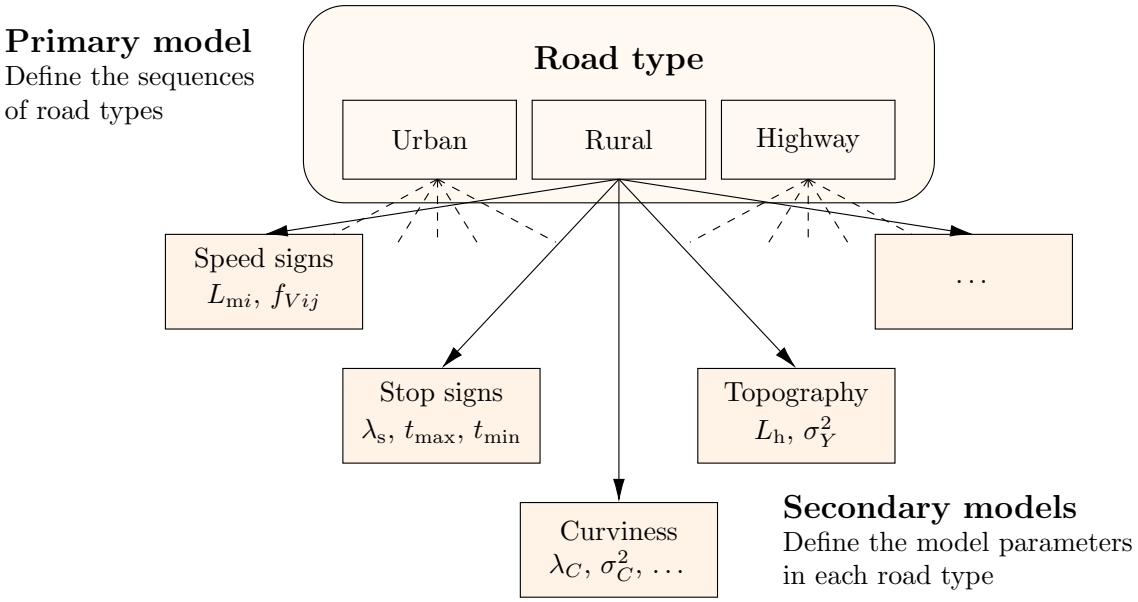

Figure 2.2: The road type is the primary road model. The other parameters are treated as ancillary and inherit their values depending on the road type. Figure adapted from Paper 1.

we postulate the existence of n_r different road types $\{r_1, ..., r_{n_r}\}$, there need to be $n_r - 1$ characteristic speeds $\{v_1, ..., v_{n_r-1}\}$, ordered in ascending magnitude. The road type r_t at any point x would then be given by the speed limit $v(x)$ at this point through

$$r_t(x) = \begin{cases} r_1, & v \leq v_1, \\ r_i, & i : v_{i-1} < v \leq v_i, \qquad i = 2, ..., n_r - 1, \\ r_{n_r} & v_{n_r-1} < v. \end{cases} \tag{2.21}$$

The road type itself becomes a piecewise constant function of the speed limit, and the speed limit sign is a piecewise constant function of the position. Therefore, the road type is modelled analogously to the speed sign, and is fully parametrised by the n_r mean lengths L_{mi} and the hollow matrix $\mathbf{F}_r \in \mathbb{R}^{n_r \times n_r}$, whose entries are elements f_{rij} similarly defined as those in Eq. (2.19).

In Fig. 2.2 a schematic of the hierarchical structure of the sOC is shown graphically for $n_r = 3$ (urban, rural and highway).

Topography

The models for topography are borrowed from Johannesson, Podgórski, and Rychlik (2017) and Johannesson, Podgórski, Rychlik, and Shariati (2016). The road is partitioned into short segments k and the road gradient $\{Y_k\}$ is treated as a random variable on each k. The topography is then modelled by using a first order autoregressive AR(1) process as follows:

$$Y_k = \phi_Y Y_{k-1} + e_{Y,k}, \qquad e_{Y,k} \sim \mathcal{N}\left(0, \sigma^2_{e_Y}\right), \tag{2.22}$$

where $\mathcal{N}$ denotes the normal distribution and ϕ_Y and σ_{e_Y} are the two characteristic parameters. The autoregression parameter ϕ_Y may be written in terms of a hill length L_h:

$$L_\mathrm{h} = \frac{4\pi}{\pi - 2\arcsin\alpha} L_\mathrm{s}. \tag{2.23}$$

The error variance σ_{e_Y} may be also expressed as a topography amplitude:

$$\sigma_Y^2 = \frac{\sigma_{e_Y}^2}{1 - \phi_Y^2}. \tag{2.24}$$

The parameters L_h and σ_Y^2 are sufficient to parametrise the topography model.

Curviness

A curve may be modelled as an independent event having a location, curvature (inverted radius) and length. Pettersson, Johannesson, et al. (2019) refer to this type of description as the *curviness* of the road and denote the sequence by $\{X_k, C_k, L_k\}$. The locations X are modelled as a Poisson process obeying Eq. (2.15), with intensity λ_C. The curvature C is modelled as a modified log-normal distribution:

$$R' = 1/C - r_\mathrm{turn}, \qquad \log R' \sim \mathcal{N}\left(\mu_C, \sigma_C^2\right), \tag{2.25}$$

with parameters λ_C, σ_C^2 and minimum curve radius r_turn. The curve length L is then modelled as a log-normal distribution of the type

$$\log L \sim \mathcal{N}\left(\mu_L, \sigma_L^2\right), \tag{2.26}$$

with parameters μ_L and σ_L^2. Together, these six values fully parametrise the curviness model.

Road roughness

The model for road roughness is not treated here and the reader is referred to Johannesson, Podgórski, and Rychlik (2016) for additional details.

2.3.3 Secondary weather models

At present, the secondary weather models include ambient temperature, atmospheric pressure, precipitation, wind velocity and relative humidity. These models have been introduced by the author in Paper 2. The major assumption is that the weather properties can be assumed to remain (approximately) constant in space. Therefore, only the explicit dependence on time is modelled.

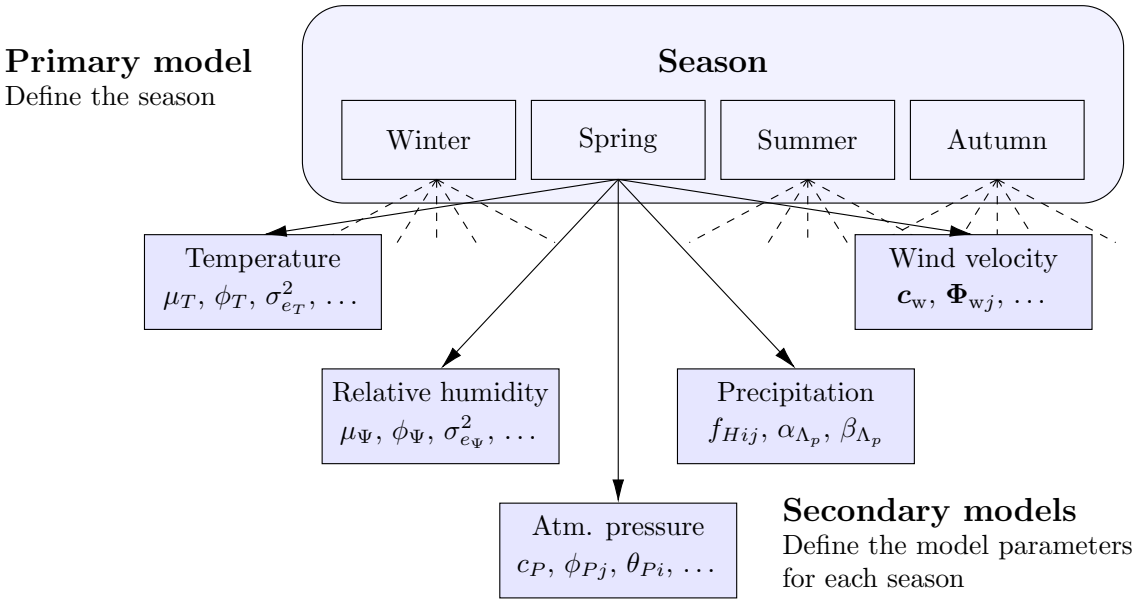

Figure 2.3: The season is the primary weather model. The other parameters are treated as ancillary and inherit their values depending on the season.

Air temperature and relative humidity

Air temperature and relative humidity exhibit seasonal trends which are deterministic in nature (Eymen and Köylü 2019; Liu et al. 2018). Therefore, for both physical quantities, whose sequences are denoted by $\{T_{\mathrm{air},k}\}$ and $\{\Psi_{\mathrm{RH},k}\}$ respectively, a distinction is made between a deterministic component (which tries to capture the diurnal and seasonal trends) and a stochastic one (which replicates the random variations occurring during the day). The complete models are thus assumed to be of the form:

$$T_{\mathrm{air},k} = \mu_T + T_\mathrm{d} \sin\Big(\omega_\mathrm{d} d_\mathrm{d}[t] + \varphi_{T_\mathrm{d}}\Big) + T_\mathrm{y} \sin\Big(\omega_\mathrm{y} d_\mathrm{y}[t] + \varphi_{T_\mathrm{y}}\Big) + \tilde{T}_k, \tag{2.27a}$$

$$\Psi_{\mathrm{RH},k} = \mu_\Psi + \Psi_\mathrm{d} \sin\Big(\omega_\mathrm{d} d_\mathrm{d}[t] + \varphi_{\Psi_\mathrm{d}}\Big) + \Psi_\mathrm{y} \sin\Big(\omega_\mathrm{y} d_\mathrm{y}[t] + \varphi_{\Psi_\mathrm{y}}\Big) + \tilde{\Psi}_k, \tag{2.27b}$$

where $\omega_\mathrm{d} = 2\pi/24$ and $\omega_\mathrm{y} = 2\pi/365$ are the daily and annual frequencies of the periodic signal, and $d_\mathrm{d}[t]$ and $d_\mathrm{y}[t]$ are the daily mod and annual ceiling operators (Liu et al. 2018), defined respectively as:

$$d_\mathrm{d}[t] = (t \bmod 24), \tag{2.28a}$$

$$d_\mathrm{y}[t] = \left\lceil \frac{t}{24} \right\rceil. \tag{2.28b}$$

In Eqs. (2.27), the quantities μ_T and μ_Ψ represent the average temperature and humidity over the year; the amplitudes T_d, T_y and Ψ_d, Ψ_y model the daily and annual deterministic trends, whilst the random variables $\tilde{T}_k$ and $\tilde{\Psi}_k$ capture the residuals (Box et al. 2015). More specifically, a simple AR(1) process is used to model the stochastic components, i.e.

$$\tilde{T}_k = \phi_T \tilde{T}_{k-1} + e_{T,k}, \qquad e_{T,k} \sim \mathcal{N}\Big(0, \sigma^2_{e_T}\Big), \tag{2.29a}$$

$$\tilde{\Psi}_k = \phi_\Psi \tilde{\Psi}_{k-1} + e_{\Psi,k}, \qquad e_{\Psi,k} \sim \mathcal{N}\Big(0, \sigma^2_{e_\Psi}\Big), \tag{2.29b}$$

where the characteristic parameters are ϕ_T, $\sigma^2_{e_T}$ and ϕ_Ψ, $\sigma^2_{e_\Psi}$.

It is worth pointing out that the deterministic components for both models are calculated over the year, and therefore the parameters μ_T, μ_Ψ, T_d, T_d, Ψ_d, Ψ_y, φ_{T_d}, φ_{T_y} and $\varphi_{\Psi_\mathrm{d}}$, $\varphi_{\Psi_\mathrm{y}}$ are independent of the seasonal settings. Conversely, the stochastic parameters ϕ_T, ϕ_Ψ, $\sigma^2_{e_T}$ and $\sigma^2_{e_\Psi}$ inherit their values from the specific season, which is the primary weather model.

Atmospheric pressure

The model for atmospheric pressure is based on that by La Rocca et al. (2010) and consists of an ARIMA(p, d, q) process:

$$\phi_P(L)(1-L)^d P_{\mathrm{air},k} = c_P + \theta_P(L) e_{P,k}, \qquad e_{P,k} \sim \mathcal{N}\Big(0, \sigma^2_{e_P}\Big), \tag{2.30}$$

where $\phi_P(L)$ is a stable degree p AR lag operator polynomial and $\theta_P(L)$ is an invertible degree q MA operator polynomial. To summarise, the model for atmospheric pressure is fully parametrised by the constant term c_P, the autoregressive coefficients ϕ_{Pj}, $j = 1, \ldots, p$, the moving average coefficients θ_{Pi}, $i = 1, \ldots, q$ and the innovation variance $\sigma^2_{e_P}$.

Precipitation occurrence and amount

The sequence for the atmospheric precipitation is modelled in a two-step process. In the first step, the occurrence of the event $\{H_{\mathrm{p},k}\}$ is simulated, and then a suitable probability distribution is used to fit the intensity $\{\Lambda_{\mathrm{p},k}\}$, which corresponds to the precipitation amount. The occurrence is modelled using a Markov chain with fixed interval length, similarly to what done in Chin (1977) and Gabriel and Neumann (1962). The stochastic variable $H_{\mathrm{p},k}$ is allowed to take states from the discrete space $\{1, 2\}$, where 1 and 2 are the labels for the *dry* and *wet* events, respectively. In analogy to Eq. (2.18), the precipitation occurrence is also assumed to satisfy the Markov property A.2.1:

$$\begin{aligned} \mathbb{P}\Big(H_{\mathrm{p},k} = h_{\mathrm{p},k} \Big| H_{\mathrm{p},1} = h_{\mathrm{p},1}, H_{\mathrm{p},2} = h_{\mathrm{p},2}, \ldots, H_{\mathrm{p},k-1} = h_{\mathrm{p},k-1}\Big) \\ \approx \mathbb{P}\Big(H_{\mathrm{p},k} = h_{\mathrm{p},k} \Big| H_{\mathrm{p},k-1} = h_{\mathrm{p},k-1}\Big). \end{aligned} \tag{2.31}$$

Furthermore, for the case under consideration, we have only two states, and hence the Markov matrix associated to the process $\mathbf{P}_H \in \mathbb{R}^{2\times 2}$ collects four entries in total. From Eq. (A.21), we may easily deduce:

$$p_{H12} = 1 - p_{H11}, \tag{2.32a}$$

$$p_{H21} = 1 - p_{H22}. \tag{2.32b}$$

Thus, only the transition probabilities p_{H11} and p_{H22} need to be estimated to completely characterise the model. The estimation may be carried out considering the two ratios

$$p_{H11} = f_{H11}/(f_{H11} + f_{H12}), \tag{2.33a}$$

$$p_{H22} = f_{H22}/(f_{H21} + f_{H22}). \tag{2.33b}$$

The interpretation in physical terms of the coefficients f_{Hij} appearing in (2.33) is quite straightforward. For example, the coefficient f_{H11} represents the number of dry intervals preceded by dry intervals, whilst f_{H12} the number of wet intervals preceded by dry ones. Therefore, the coefficient f_{Hij} are used to parametrise the precipitation occurrence, since they are easier to understand.

Finally, when the wet event occurs a Gamma distribution is used to model the intensity of the precipitation (Husak et al. 2007; Kumar et al. 2017):

$$\Lambda_{\mathrm{p},k} \sim \mathrm{Ga}\Big(\alpha_{\Lambda_\mathrm{p}}, \beta_{\Lambda_\mathrm{p}}\Big). \tag{2.34}$$

The precipitation model is hence described fully by the coefficients f_{Hij} and the shape and rate parameters $\alpha_{\Lambda_\mathrm{p}}$ and $\beta_{\Lambda_\mathrm{p}}$.

Wind speed and direction

For wind modelling, different approaches have been proposed in the literature, including hybrid and complex multivariate formulations (Cadenas et al. 2016; Hocaoğlu et al. 2010). The main complication when dealing with this parameter is that wind speed and direction often exhibit a strong correlation. Hence, the two signal need to be modelled properly by taking into account their mutual interaction. A natural (and simple) possibility is to resort to a VAR model, which extends the standard notion of an autoregressive series by coupling different random processes. It may be written:

$$\boldsymbol{\Phi}_\mathrm{w}(L)\boldsymbol{Y}_{\mathrm{w},k} = \boldsymbol{c}_\mathrm{w} + \boldsymbol{e}_{\mathrm{w},k}, \tag{2.35}$$

where the vector $\boldsymbol{Y}_{\mathrm{w},k} = \begin{bmatrix} V_{\mathrm{w},k} & \Theta_{\mathrm{w},k} \end{bmatrix}^\mathrm{T}$ collects the wind speed $V_{\mathrm{w},k}$ and direction $\Theta_{\mathrm{w},k}$ at each discrete time step k, the parameter $\boldsymbol{c}_\mathrm{w} \in \mathbb{R}^2$ represents a constant offset and $\boldsymbol{e}_{\mathrm{w},k} \in \mathbb{R}^2$ is the vector of normally distributed innovations with covariance matrix given by $\boldsymbol{\Sigma}_{\boldsymbol{e}_\mathrm{w}} \in \mathbb{R}^{2\times 2}$. Finally, the matrix operator $\boldsymbol{\Phi}_\mathrm{w}(L)$ reads

$$\boldsymbol{\Phi}_\mathrm{w}(L) = \mathbf{I} - \sum_{j=1}^{p} \boldsymbol{\Phi}_{\mathrm{w}j} L^j, \tag{2.36}$$

in which every $\boldsymbol{\Phi}_{\mathrm{w}j} \in \mathbb{R}^{2\times 2}$ is a matrix of AR coefficients. An intermediate step is needed for the wind direction, which is a circular variable. This require the knowledge of the mean wind direction μ_{Θ_w}. Further details are are given in Erdem and Shi (2011) and Fisher (1993). To summarise, the wind model is fully described by the average direction μ_{Θ_w}, the constant term $\boldsymbol{c}_\mathrm{w}$, the error covariance matrix $\boldsymbol{\Sigma}_{\boldsymbol{e}_\mathrm{w}}$ and the autoregressive matrices $\boldsymbol{\Phi}_{\mathrm{w}j}$, $j = 1, \ldots, p$.

2.3.4 Secondary traffic model

Average characteristics of vehicular traffic are important when it comes to assessing energy efficiency (Sciarretta 2020). The customary approach consists of describing traffic by

means of macroscopic variables. The three main variables to consider are the traffic density $\rho_{\mathrm{t}}(x,t)$, expressed as a number of vehicles per distance, the traffic speed $v_{\mathrm{t}}(x,t)$, and the traffic flow $q_{\mathrm{t}}(x,t) = \rho_{\mathrm{t}}(s,t)v_{\mathrm{t}}(x,t)$, usually measured in number of vehicles per unit of time.

The secondary traffic model has been developed in Paper 2 under the assumption of stationary flow. In this case, density and speed are correlated, and thus only one independent variable is needed to completely describe the traffic state. In our case, the chosen quantity is the traffic density. This is characterised by a deterministic diurnal component and thus, for each combination of road type, speed sign and season, the sequence $\{\rho_{\mathrm{t},k}\}$ is modelled as follows:

$$\rho_{\mathrm{t},k} = \mu_\rho + \rho_{\mathrm{d}} \sin\Big(\omega_{\mathrm{d}} d_{\mathrm{d}}[t] + \varphi_{\rho_{\mathrm{d}}}\Big) + \tilde{\rho}_k, \tag{2.37}$$

where μ_ρ is the average density on a specific road segment during the season, ρ_{d} is the amplitude of the daily variation, $\omega_{\mathrm{d}} = 2\pi/24$ is again the the daily frequency, $\varphi_{\rho_{\mathrm{d}}}$ the initial phase and $\tilde{\rho}_k$ represents the stochastic component. For the latter, a simple AR(1) process is used, i.e.

$$\tilde{\rho}_k = \phi_\rho \tilde{\rho}_{k-1} + e_{\rho,k}, \qquad\qquad e_{\rho,k} \sim \mathcal{N}\Big(0, \sigma^2_{e_\rho}\Big). \tag{2.38}$$

Assuming the traffic to be stationary and homogeneous on each road segment between the two discrete times k and $k+1$, an equilibrium relationship between the traffic density and speed may be then postulated in the form $v_{\mathrm{t}}(x,t) = v_{\mathrm{e}}(\rho_{\mathrm{t}}(x,t)) = f(\rho_{\mathrm{t}}(x,t))$. The relationship $v_{\mathrm{e}}(\rho_{\mathrm{t}}(x,t)) = f(\rho_{\mathrm{t}}(x,t))$ constitutes the so-called fundamental diagram of the traffic flow and is specifically given for a road type. In the literature, different possible models have been proposed to capture the dependency of the equilibrium speed on the traffic density, mostly based on empirical fitting (see Kessels (2019) for an introduction). Specifically, the simplest possible model, known as Greenshield's fundamental diagram, yields

$$v_{\mathrm{e}}\Big(\rho_{\mathrm{t}}(s,t)\Big) = v_{\mathrm{f}}\left(1 - \frac{\rho_{\mathrm{t}}(s,t)}{\rho_{\mathrm{c}}}\right), \tag{2.39}$$

where v_{f} represents the *free-flow* speed, i.e. the traffic speed corresponding to have almost no vehicle on the road, and ρ_{c} is the *critical density*. Equation (2.39) has been used in Paper 2, but other choices are also possible. However, if more complex formulations are preferred, the number of parameters might increase. Assuming Eq. (2.39) for the equilibrium relationship, the traffic density model is described completely by the parameters μ_ρ, ρ_{d}, $\varphi_{\rho_{\mathrm{d}}}$ and $\sigma^2_{e_\rho}$, which are function of both the road type and season, and the *fundamental* ones v_{e} and ρ_{c}, which only vary depending on the road properties.

The stochastic models for road, weather and traffic are finally summarised in Tab. 2.1.

2.4 The deterministic operating cycle

Compared to the first two types of representation already discussed, the deterministic operating cycle (dOC) describes the mission and the external environment with higher

Table 2.1: Summary of sOC parameters.

Model	**Category**	**Model type**	**Number of states**	**Number of parameters**
Road type	Road	Markov process	n_r	n_r^2
Stop signs	Road	Marked Poisson	Continuous	3
Give way signs	Road	Marked Poisson	Continuous	5
Traffic lights	Road	Marked Poisson	Continuous	5
Speed bumps	Road	Marked Poisson	Continuous	3
Speed signs	Road	Markov process	n_v	n_v^2
Topography	Road	Gaussian AR(1)	Continuous	2
Curviness	Road	Marked Poisson	Continuous	6
Road roughness	Road	Laplace AR(1)	Continuous	2
Temperature	Weather	Deterministic Gaussian AR(1)	Continuous Continuous	5 2
Relative humidity	Weather	Deterministic Gaussian AR(1)	Continuous Continuous	5 2
Atmospheric pressure	Weather	Gaussian ARIMA(p, d, q)	Continuous	$2 + p + q$
Precipitation	Weather	Markov process Gamma distributed	2 –	4 2
Wind speed and direction	Weather	Gaussain VAR(p)	Continuous	$6 + 4p$
Traffic density	Traffic	Deterministic Gaussian AR(1)	Continuous Continuous	5 2

accuracy. The dOC is the most adequate way of modelling an operating cycle when it comes to simulation. The central idea is that it may serve as a virtual environment for realistic prediction of road vehicles performance, virtual testing and design of control algorithms and development of *ad-hoc* functions.

In the dOC, the same four different categories defined for the sOC, namely the road, traffic, weather and mission, are kept. For each of them, a different set of parameters is used. These correspond to the physical quantities which were regarded as *models* in the sOC representation[8], and are defined as discrete functions of time and position. Some parameters are only made dependent on either the position or the time, some others, like the ones marked in the traffic category, depend on both. Additionally, each parameter may be represented by a scalar or a vector-valued signal (see dimensionality in Tab. 2.2). Any value in between two different discrete times (or positions) may be computed by interpolation using the corresponding model in Tab. 2.2. For the motivation behind the choice of the specific interpolation strategy for individual parameters, the reader is referred to Pettersson, Berglund, et al. (2019). To formalise the dOC format mathematically, the four categories (see Tab. 2.2) may be defined as the sets containing the parameter

[8]The relationship between the role of a physical quantity in the sOC and dOC representations is perhaps better understood from Tab. 2.2, where each entity is labelled under *model* for the sOC and *parameter* for the dOC.

Table 2.2: Stochastic (secondary) models and deterministic parameters (dOC parameters) for the sOC and dOC representations. *Linear* and *constant* refer to linear and right-side continuous piecewise constant interpolation models, respectively. The mathematical model of *Dirac delta* occurs when the parameter is regarded as an isolated *event*.

Model or parameter	**Category**	**Type**	**Interpolation model**	**Dim**	**Quantity**
Speed signs	Road	Function	Constant	1	Speed limit
Altitude	Road	Function	Linear	1	Vertical coordinate
Curvature	Road	Function	Linear	1	Curvature
Ground type	Road	Function	Constant	2	Surface type, cone index
Roughness	Road	Function	Constant	2	Waviness, roughness coeff.
Stop signs	Road	Event	Dirac delta	1	Standstill time
Traffic lights	Road	Event	Dirac delta	1	Standstill time
Give way signs	Road	Event	Dirac delta	1	Standstill time
Speed bumps	Road	Event	Dirac delta	3	Length, height angle of approach
Longitude	Road	Function	Linear	1	WGS84 longitude
Latitude	Road	Function	Linear	1	WGS84 latitude
Ambient temperature	Weather	Function	Linear	1	Temperature
Atmospheric pressure	Weather	Function	Linear	1	Pressure
Precipitation	Weather	Function	Constant	1	Precipitation amount
Wind velocity	Weather	Function	Constant	2	Velocity vector
Relative humidity	Weather	Function	Linear	1	Humidity
Traffic density	Traffic	Function	Constant	1	Density
Mission stops	Mission	Event	Dirac delta	1	Standstill time
Cargo weight	Mission	Function, event	Linear, constant	1	Payload
Power take-off	Mission	Function	Linear	1	Output power
Charging power	Mission	Function	Constant	1	Input power
Travel direction	Mission	Function	Constant	1	Driving direction

sequences: $\mathcal{R}_\mathrm{d}$ is the set containing all sequences labelled as road, $\mathcal{W}_\mathrm{d}$ for weather, $\mathcal{T}_\mathrm{d}$ for traffic and $\mathcal{M}_\mathrm{d}$ for mission. Then, the dOC format may be defined mathematically as the collection of sets:

$$\mathcal{OC}_\mathrm{d} = \{\mathcal{R}_\mathrm{d}, \mathcal{W}_\mathrm{d}, \mathcal{T}_\mathrm{d}, \mathcal{M}_\mathrm{d}\}, \tag{2.40}$$

and interpolation may be defined as an operator acting on the elements in the sets. However, Eq. (2.40) is only an elegant formalism: it describes the dOC as an algebraic structure, but does not bring much more information about it. The deterministic parameters are simply defined on different spaces, where the relative interpolation operators are allowed to act.

The dOC format provides a detailed view on individual transport operations without making any assumptions about the driver or the vehicle. Furthermore, it is built in a modular way such that parameters may be easily modified, added or removed. To be useful in simulation, the dOC format must be integrated with suitable dynamic models for vehicle and driver. In the context of this thesis work, this has been done by resorting to the VehProp environment, which is an open platform[9]. This has been firstly conceived by

[9]Available from: http://www.chalmers.se/en/departments/m2/research/veas/Pages/VehProp.aspx.

Jacobson et al. (n.d.) and then further extended by Pettersson and the author himself to support the dOC framework. A detailed description of VehProp is beyond the scope of this thesis, but it might be beneficial to briefly comment on how the dOC parameters may be used in practice to reflect variation in usage. A straightforward way to consider the influence from the different physical entities listed in Tab. 2.2 is to use an interpretative driver model, which reacts to the external stimuli and sets his reference speed accordingly. This idea, borrowed from Eriksson (1997) and Michon (1985), has been refined by Pettersson (2019). In this context, the complete set of functions currently used to feed the driver model is listed in Pettersson (ibid.) and not reported here for brevity. Limiting ourselves to an illustrative example, we shall refer to Eq. (2.39) to account for variation in (desired) speed due to external traffic conditions. Looking at the structure of Eq. (2.39), it becomes obvious that the driver's reference speed reduces as the vehicular density increases. An analogous reasoning may be extended to any dOC parameter which correlates with a corresponding target speed, provided that a suitable model has been formulated.

2.5 Relationship between the representations

The three levels of representation discussed so far are intrinsically related, and ordered in a pyramidal structure, as shown graphically in Fig. 2.4.

The first connection which we shall explore is that between the bird's eye view and the sOC. They are both statistical descriptions, but with considerably different resolution. Indeed, whilst the bird's eye view is mainly limited to encompass an entire transport application, the sOC targets individual missions. The formal relationship existing between the two levels may be clarified by looking at the GTA classes introduced previously. With the topography as an example, it is possible to estimate the process variances which yield the thresholds set by the GTA classification system. The calculations have been carried out by Pettersson, Johannesson, et al. (2019) and are not reported here, but the results are listed in Tab. 2.3. Given an sOC, we may thus deduce the corresponding GTA class

Table 2.3: Equivalence between GTA topography class and topography amplitude in the sOC description.

Variance	**GTA class**
$\sigma_Y^2 < 1.66$	`FLAT`
$1.66 \leq \sigma_Y^2 < 6.65$	`P-FLAT`
$6.65 \leq \sigma_Y^2 < 14.98$	`HILLY`
$14.98 \leq \sigma_Y^2$	`V-HILLY`

directly by inspection of Tab. 2.3. The inverse operation is not possible since, for a predetermined GTA class, there exist infinite different sOCs. This kind of non-bijective relationship in the descending direction also persists at the lower level between the sOC and dOC representations. Indeed, a dOC may be interpreted as a single realisation of an sOC, given a set of stochastic parameters. Two dOCs originating from the same sOC are thus equivalent in a statistical sense, but can be significantly different in practice. This implies again that the map between an sOC and a dOC is never bijective. The relationship in the opposite direction is simple to grasp: given a dOC, it is possible to estimate the

corresponding stochastic parameters and hence obtain an equivalent description in terms of an sOC, as illustrated also in Fig. 2.4. The connection between the sOC and dOC

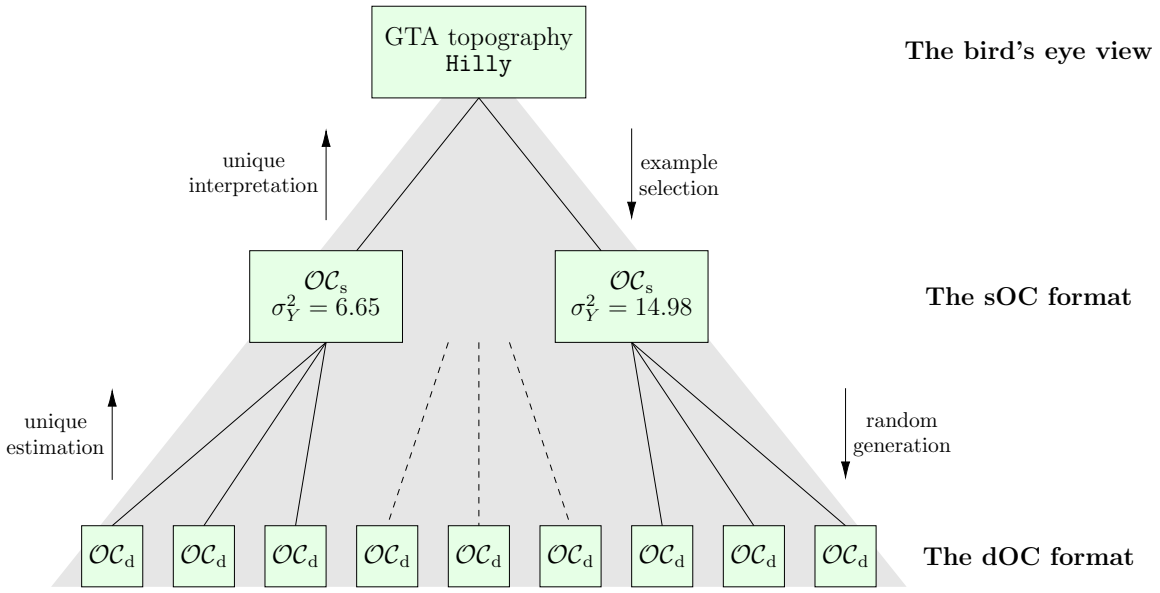

Figure 2.4: Schematic representation of the pyramidal structure of an OC. All the missions being equivalent in the sense of a GTA class belong to the same transport application (the bird's eye view). The individual statistical properties may however differ within the transport application (sOC). Finally, transport missions can be statistically equivalent but significantly different in practice. This is captured by the dOC representation.

descriptions plays a fundamental role in product development and selection, since an sOC may be translated into a multitude of deterministic representations. This is done by generating synthetic dOCs whose parameters are interpreted as individual realisations of the corresponding stochastic models. In turn, each dOC may be used in combination with virtual models for vehicle and driver, allowing for accurate prediction, design optimisation and function development.

Chapter 3

A case study in product selection

We have outlined the theoretical foundation of the operating cycle format, and the relationships existing between the three levels of representation. Conceptually, the edifice constructed so far seem to be solid and well-grounded, but its concrete potential still deserves to be exemplified. The applicability of the OC description extends to a wide variety of applications, spacing from theoretical studies, like pure optimisation, to more practical situations requiring a strict interaction between the stakeholders. In this context, the aim of the present chapter is to illustrate how the OC framework can be used in practice. Optimisation problems cover a domain which is immensely vast *per se*, and the benefits of using the OC descriptions are not explored here. Instead, we shall consider the simpler example of product selection. The following discussion retraces what already investigated in Paper 1.

3.1 Background

Let us think of a road operator which is mainly active in the construction sector within a large area around Göteborg, Sweden. The owner needs to purchase a new vehicle. The current truck is a Volvo FH16 750, and is mainly used to load and unload gravel, and often it comes equipped with a trailer. In replacing the current vehicle, the road operator aims at saving as much fuel as possible and minimising the emissions. The candidate vehicles are another (identical but new) Volvo FH16 750, and a Volvo FH13 540, equipped with a smaller engine. The complete specifications of both configurations are not reported here for brevity, but can be found in the Volvo datasheets[1].

From February to May 2020, the truck delivers a bunch of files logged during its daily transport operations, covering a wide spectrum of road missions, with different characteristics. The log data collected from the truck can be converted into mathematical descriptions, statistical or deterministic, as already explained in Chap. 2. This conversion may be carried out sequentially, starting with the bird's eye view description which is used to select reference transport applications. These are translated into a dOC, and then back again to the upper hierarchical level into an sOC. From the sOC description,

[1] Available from: https://www.volvotrucks.se/sv-se/trucks/trucks/volvo-fh16/specifications/data-sheets.html.

new transport missions – in the form of synthetic dOCs – may be generated which share the same statistical properties of the original one. This enables to create a statistical representation of the vehicle usage, which may be employed to investigate both usage and variation.

Once a mathematical description of a road transport mission is available, a comparison amongst different vehicle designs may be made to assess their performance. In our case, the aim is to investigate which configuration – FH16 750 or FH13 540 – exhibits lower fuel consumption and the CO_2 emissions, given a known dataset of road operations.

In the *iter* outlined above, the most delicate part is perhaps to carefully select the reference missions such that they are representative of the overall usage. From a statistical viewpoint, this translates into the more formal problem of finding suitable metrics and thresholds which completely describe the transport application. Another aspect to consider is that the classification problem grows with combinatorial complexity. Therefore, it may be beneficial to systematically exclude from the analysis those parameters which are expected to only have a small influence upon the identified metrics. In some cases, as in Paper 1, an heuristic approach might eventually be preferred, but more scientific ways of selecting such missions should also be explored.

In the following we will explain how to take advantage of the three levels of representation – the bird's eye view, the sOC and the dOC – to fully characterise the transport application in a simple and efficient way.

3.2 A three-level description

The first step should consist of a preliminary analysis about the statistical distribution of the available road missions. This allows to identify a restricted number of transport applications, to which the vehicle's design may be tailored.

The brid's eye view and the sOC play both a major role in this process. As already discussed, there exists a non-bijective relationship between the two levels of descriptions, which enables to classify a transport mission based on its statistical properties. As an example, let us consider only three parameters, as done in Paper 1: road grade, mission length and duration (in time). With reference to the first property, it has been shown that, when an AR(1) process is used to model to topography, each GTA class sets lower and upper bounds only on the variance σ_Y^2. Therefore, estimating the value of σ_Y^2 for a mission is automatically equivalent to label it under one of the classes listed in Tab. 2.3. This can be done also for the other parameters, resulting into a matrix which condenses the statistical properties of different transport applications.

In Tab. 3.1, the final distribution from 163 files delivered by the truck operator are grouped into a matrix-like fashion. An alternative (graphical) representation is illustrated in Fig. 3.1, together with three selected reference missions.

From Tab. 3.1, it emerges that, for the case-study under consideration, there is approximately the same number of `P-FLAT` and `HILLY` missions, whereas the `V-HILLY` missions are slightly fewer. Recalling the example of Paper 1, it seemed legitimate to select one mission from each topography class. Furthermore, the first cell, i.e. the cell with the shortest distance and duration, is the mode cell for all classes and thus a reference mission

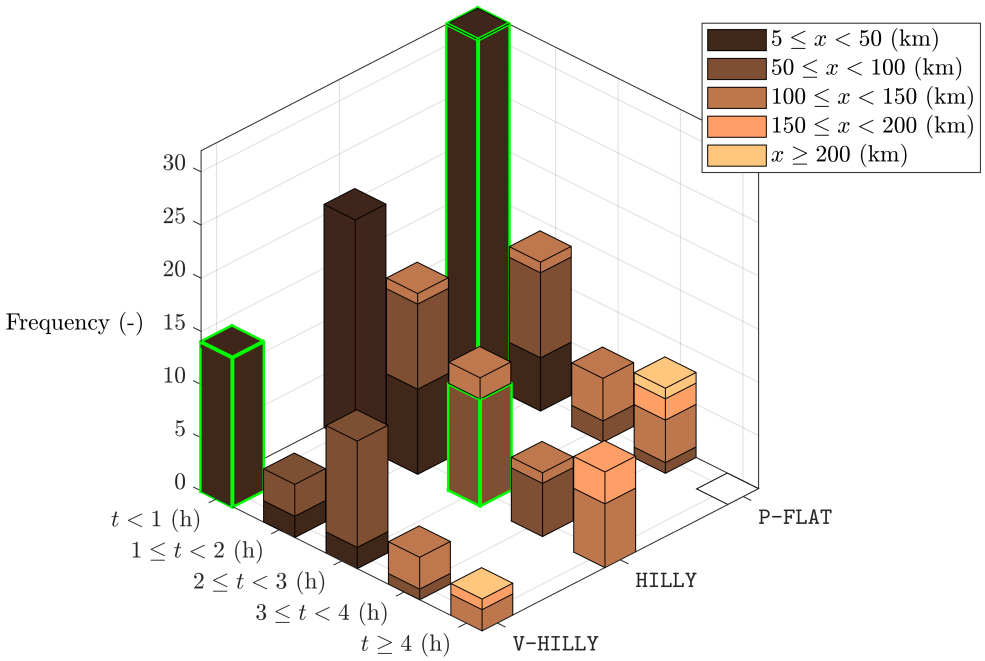

Figure 3.1: A 3D stacked bar chart displaying the mission distribution based on the classification description. A mission have been picked from each suggested bar marked in green. Figure adapted from Paper 1.

Table 3.1: Characteristics of the reference missions.

	Mission 1	Mission 2	Mission 3
Topography:	`V-HILLY`	`HILLY`	`P-FLAT`
Distance:	39 km	67.2 km	17.4 km
Duration:	0.9 h	2.15 h	0.6 h

from that combination was also picked. The corresponding blocks are highlighted in light green in Fig. 3.1.

Once the reference missions have been selected, the corresponding dOCs can be built starting from the deterministic models listed in Tab. 2.2. The estimation procedure for the sOC parameters might differ considerably depending on the category. For some parameters, like topography and curvature, the estimation may be carried out starting from available signals measured by on-board sensors using the WAFO[2] package implemented in MATLAB®. This approach is the one also followed in ibid. and in Paper 1.

On the other hand, the extraction of parameters like legal speed, stop sign, traffic light and give way sign must be usually retrieved manually. Analogously, detailed information about weather and traffic conditions is often not available directly from log data, and must be supplemented using external sources. This can be certainly done if the GPS coordinates and the exact daytime of the mission are known. The most intuitive and simple choice is

[2]Available from: `http://www.maths.lth.se/matstat/wafo/`.

perhaps to resort to external databases which offer data free to download. Some examples are the SMHI service[3] and Trafikverket database[4], which collect weather and traffic data at a fixed time resolution (usually one hour). This is particularly practical when it comes to analysing transport operations which take place within a well-defined geographical area, for which the weather parameters can be assumed remain approximately constant. If the road operations extend into a larger area, an option is to build a weather map by combining information collected from several station. The practical aspects connected with the parametrisation of the weather and traffic models are omitted here for brevity, but discussed extensively in Paper 2.

For each fully parametrised dOC, there is an equivalent statistical description in the form of an sOC, as already explained in Sect. 2.5. The relationship between the dOC and sOC representations is injective the ascending direction, and therefore a unique set of sOC parameters can always be determined starting from a given dOC. This allows to construct new sequences by generating random numbers from known probability distributions. Figure 3.2 illustrates schematically the typical workflow which synthesises a reference dOC starting from the corresponding statistical description.

The primary models for road and weather are firstly generated over a specified mission distance, which is prescribed by the user and later on included amongst the mission parameters. To allow for fair comparison, the mission length may be defined so as to match the original distance travelled by the vehicle in the reference mission. The number of days to be simulated is another input to the process, which accordingly generates the weather and traffic timeseries over a finite horizon. For this operation, the time resolution must be the same as the one used to parametrise each sOC model. The primary models are also generated simultaneously, since no explicit interaction is expected between the primary weather and traffic categories. It is worth mentioning that, whilst the overall road consists of a sequence of road types, the season can be generally assumed to be constant over the mission. Both models are simulated depending on their stationary distribution, which may be deduced from the models introduced in Sect. 2.3. Finally, the timeseries for the secondary models are simulated. This step is carried out using again the *ad-hoc* WAFO package and the Econometric Toolbox[5]. The sequences obtained by means of this procedure need to be converted into the dOC language. For example, curvature and topography are translated into curviness and altitude; similarly, wind speed (in magnitude) and direction are instead reformulated in terms of velocity vector, where the components are specified. Furthermore, the wind speed is usually measured at weather stations at approximately 10 m above the ground, and therefore the value must be converted to ground level. This usually done employing empirical relationships such as the logarithmic speed profile (Tennekes 1973). From the signed curvature, the actual road profile and the tangent vector to the trajectory are also deduced by numerical integration. This step is crucial since it allows to compute the relative direction between the vehicle and the wind velocity vector. The dOC parameters, plus their location in either space or time (or both for the traffic density), are finally encoded in the dOC description and tabulated.

[3]Available from: https://www.smhi.se/en/weather/sweden-weather/observations#ws=wpt-a,proxy=wpt-a,tab=vader,param=t.

[4]Available from: https://vtf.trafikverket.se/SeTrafikinformation.

[5]Available from: https://se.mathworks.com/products/econometrics.html.

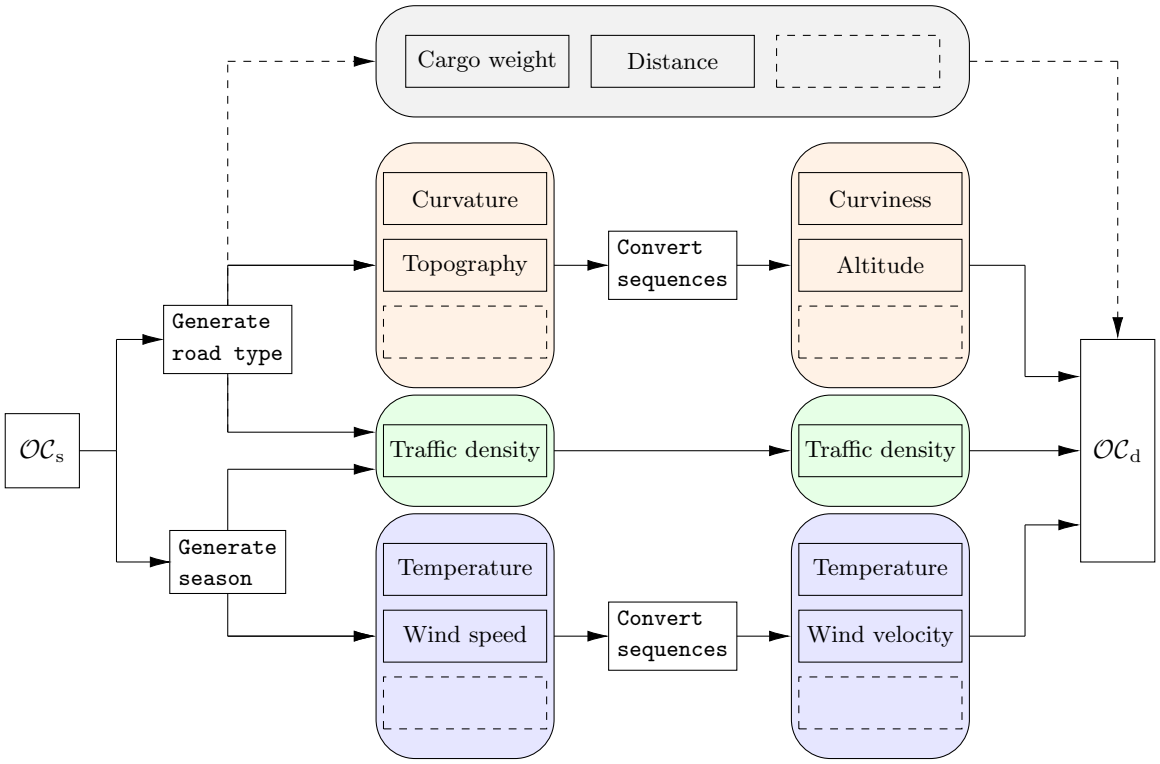

Figure 3.2: Process of generation of a deterministic operating cycle (dOC) from a stochastic one (sOC). The mission category is assigned *a priori* and matches the characteristics of the reference dOC. All the other models are generated stochastically. It must be noticed that a conversion is needed between the sOC models and the corresponding dOC parameters. Figure adapted from Paper 2.

In Paper 1, 200 new cycles (which we can think of as individual realisation) were generated from each sOC, summing up to 600 synthetic missions in total. The dOCs were also mirrored to ensure the preservation of the total potential (gravitational) energy.

3.3 Simulation results

The dOCs (either original or synthetic) may be used as an input to a complete simulation model for longitudinal vehicle dynamics, for example the already mentioned VehProp environment (Pettersson, Jacobson, et al. 2016). This allows for straightforward comparison between different configurations, in our case the two trucks FH16 750 and FH13 540. In the example taken from Paper 1, the chosen metric was the fuel consumption, expressed as $\mathrm{l}\,10^{-1}\mathrm{km}^{-1}$[6].

Here we adopt the same criterion for comparison. The distribution in performance may be obtained by considering the output from each simulated dOC as a different realisation of the process, as represented schematically in Fig. 3.3. In this context, it is expected that different vehicle designs produce different distributions of fuel consumption. Simulation

[6] 10 km correspond to one Swedish mil.

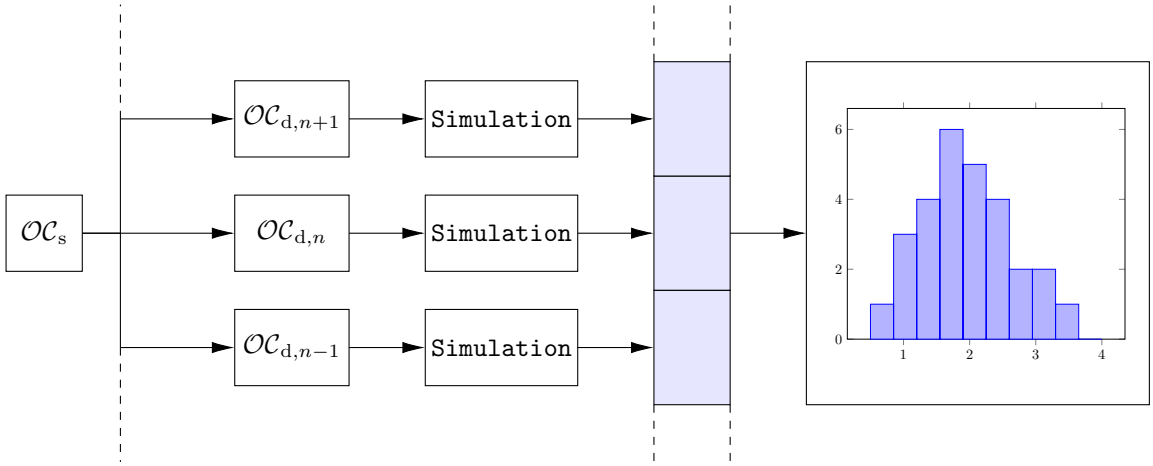

Figure 3.3: A stochastic operating cycle (sOC) can be used to synthesise different deterministic realisations (dOCs) which share the same statistical properties. The distribution in fuel consumption produced by a specific combination of sOC parameters and vehicle's specification can be evaluated by simulating each dOC and clustering the output data. Figure adapted from Paper 2.

results confirm this prediction, as it may be observed by looking at Fig. 3.4, where the histograms refer to the numbers originating from the synthetic operating cycles. These are modelled exactly in the same way, without any kind of contamination from the vehicle itself. Generally speaking, it was possible to conclude that the FH13 540 (orange histograms) outperforms the FH16 750 (blue histograms) in terms of energy efficiency. In particular, the mean value μ is lower for the FH13 540 for all the reference missions. In the case study of Paper 1, it could then be concluded that, using the fuel consumption as unique metric for comparison, the FH13 540 configuration would be preferable to purchase. There are of course, other important criteria to consider when comparing the two trucks. These were accounted also for in Paper 1.

The example presented in this chapter demonstrates that the simulation concept with the OC format can work in practice. It also shows that each level of description fulfills its own function: the bird's eye view can be used as a classification method to group individual missions into transport applications; the sOC representation allows to predict any spread in performance which can be expected depending on the vehicle design; the dOC description is the natural connection between the abstract model and the real operation, and serves as main tool for both estimation and validation purposes.

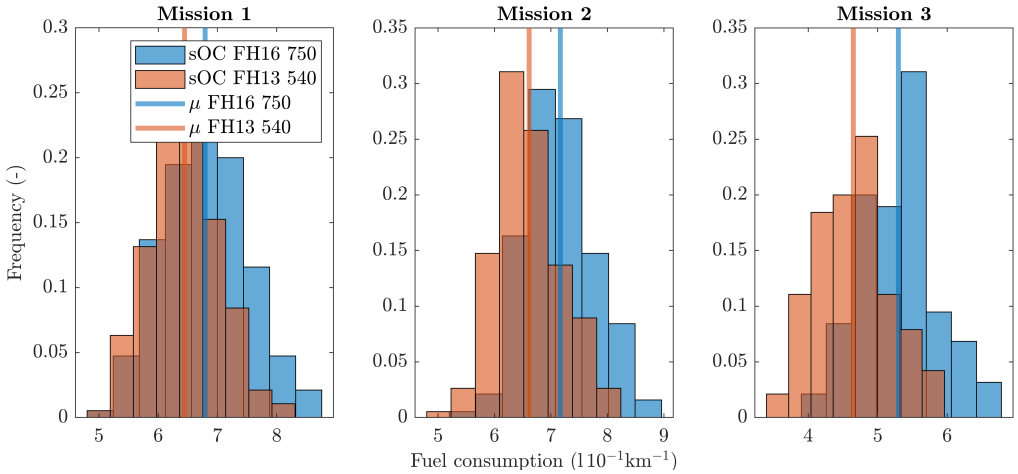

Figure 3.4: Dual histogram of the generated mission distributions for fuel consumption for both trucks. Blue: FH16 750; orange: FH13 540. Figure adapted from Paper 1.

Chapter 4

Discussion, conclusions and future research

In this chapter we summarise the main results of the thesis, with an outlook to future research.

4.1 Discussion and conclusions

In the introduction, two main research objectives were identified. The first was related to the pure representation problem and was mainly theoretical in nature; the second concerned the practical usefulness of the OC description, in conjunction with its concrete applicability.

To address the first issue, we have extended the OC format to include new stochastic parameters for the weather and traffic categories. These have been introduced in Paper 2 and discussed in more general terms in Chap. 2. To establish a continuity with the original sOC formulation, simple autoregressive models have been preferred. The outcome is an enriched collection of stochastic models and parameters, which can be used to describe the statistical properties of a transport mission. The enhanced framework has been conceived to allow for modularity, and to preserve the mutual independence between the preexisting road model and the new ones. At the same time, parsimony has been achieved by defining a new primary model for the weather category: seasonality. In this way, it has been possible to introduce a high level of diversification without resorting to complicated multivariate formulations.

Starting from the novel sOC description, synthetic operating cycles may be generated which are able to reproduce dynamically the weather and traffic characteristics. These may be used as a virtual environment for detailed vehicle dynamics simulations. An investigation on the effect of the weather and traffic settings on the vehicle's performance has been presented in Paper 2. More specifically, a categorical analysis has been made to assess the influence from seasonality and traffic regime (free or congested) on the CO_2 emissions. It has been shown that both factors play a major role in determining the vehicle's response, but simulations results have not been corroborated experimentally. The principal reason for which the study has been limited to the theoretical domain is that

information about weather and traffic conditions is generally not available from log-data, and needs to be supplemented from external databases.

The main goal of the second part of the thesis was to illustrate how the framework can be used when it comes to practical applications. The potential of the OC format was exemplified in a real-world case-study, where all the three levels of descriptions were employed to different purposes. More specifically, both the bird's eye view and the sOC representation were used to address the need for classification. In fact, the strategy presented in Paper 1 heavily relied on the natural connection between the two levels of description. Metrics and labels were firstly borrowed from an already existing classification system (the GTA), and then used to group individual missions into larger classes of transport applications. This allowed to considerably reduce the complexity of the problem.

At a lower-level, the non-bijective relationship between the sOC and dOC descriptions was used to synthesise a large number of operating cycles starting from few carefully selected missions. These dOC were statistically equivalent, but very different in practice. This intrinsic variation was obviously reflected in the distribution in the vehicle's performance. In Paper 1, a comparison between two different truck configurations prospected a potential saving in fuel consumption (around 10%) for the road operator.

In the case study, the simulation results found a robust confirmation from the experimental data.

Another topic which has been investigated in Paper 3, but only briefly touched upon in this thesis, relates directly to the physical principles which cause energy loss during the vehicle's motion. In particular, the analysis conducted in Paper 3 dealt with the friction mechanisms taking place at the tyre contact patch. It was shown that the common approach which estimates the related energy losses by multiplying the longitudinal forces for the corresponding tyre sliding speeds may be fallacious when severe transients occur. The phenomenon is rather complex, and deserves to be explored fully.

4.2 Future research

Thus far, this thesis may appear to be an apology of the operating cycle description. Quite the contrary, it should be regarded instead as a constructive criticism to the OC concept. Indeed, there are still numerous issues to tackle, and enormous margins of improvement.

To start, one of the greatest limitation of this work is connected with the obvious lackness of a scientific, exhaustive method to classify road transport missions. The duality between the bird's eye view and the sOC has been explored to a large extent, but it is still unclear whether this approach is generally good, or can be significantly improved. The metrics and labels used so far have been demonstrated to be representative of variations in usage, but this is not necessarily reflected upon variations in performance. One obvious example is the mission length: the total fuel consumed during a trip clearly increases with the travelled distance, but the fuel consumption is measured per unit of length. Besides, Pettersson (2019) has shown analytically that the expected fuel consumption is invariant with respect to the mission length. This may eventually suggest to exclude the distance from the panorama of useful indicators. Similar considerations might be valid for other parameters, which anticipate the opportunity of greatly reducing the combinatorial dimension of the problem.

How to choose metrics and thresholds is an open and interesting question. One choice could be to formalise it as an optimisation problem, and then solve it analytically or numerically. There are different mathematical tools to do that, and different directions may be explored.

Descending the hierarchical ordering of OC representations, another intriguing option concerns the stochastic modelling of the mission properties. So far, statistical models have been introduced almost exclusively for the road, weather and traffic categories. A first attempt to develop an equivalent description for the mission properties has been made by Nordström (2020), but only a limited number of features is available at present. With few exceptions (Kivekäs, Vepsäläinen, and Tammi 2018; Kivekäs, Vepsäläinen, Tammi, and Anttila 2017), stochastic approaches are not common in this context, and therefore this could potentially represent a research topic even in isolation. Furthermore, there is the tangible risk that stochastic models for the mission cannot be developed to be completely independent on the vehicle itself. Indeed, whilst the road, the weather and the traffic are separate entities which exist before the transport operation, vehicles are developed with a specific purpose in mind. From this perspective, the problem complicates soon when considering that the mission properties should probably be estimated from log-data, implying unavoidably some sort of contamination. The question seems to be rather delicate, and dedicated approaches may be required to overcome these difficulties. Eventually, the same building principles of the OC description might contrast with the need for a stochastic modelling of the mission. Another important add-on to the current version of the framework include the external infrastructure, *in primis* fuel and charging stations. Whether to include these features amongst the road parameters is debatable, but the need for stochastic models is quite obvious, especially in conjunction with the possibility of using the OC format for optimisation analyses (see e.g. Ghandriz 2018, 2020; Ghandriz, Hellgren, et al. 2016; Ghandriz, Jacobson, Laine, et al. 2020).

In respect to the dOC description, there are several chances of improvement. All the vehicle models used in this thesis are in fact very simple, with a reduced number of components. There is nothing really new in this direction however, and the development of more realistic models should definitely not represent the true core of future research. The driver constitutes perhaps the unique exception. At present, the model is split into a tactical and operational part. The former interprets the external stimuli coming from the environment, and translates them into a desired speed input. Mathematical relationships have been derived only for some dOC parameters (curviness, speed bumps, legal speed, traffic density), but other factors might be influential as well. We can think, for example, to precipitation amount: a driver may prefer to travel slower in case of heavy rain. Understanding the correlation existing especially between some weather parameters and the speed set by the driver is an involving task. It can be anticipated that some relationships will need to be established starting from empirical evidence rather than deductive principles. In this context, it would be crucial to collect large amount of data to make statistical inference, or to perform dedicated experiments. Virtual settings built in a driver simulator are mainly effective to study the influence from road parameters, but other approaches could be advantageous when it comes to weather or traffic. A preliminary effort has been already made in this sense, but both aspects need to be explored more in detail.

The operational module of the driver is instead based a simple PID controller, which tries to replicate the human behaviour during normal driving conditions. A possible direction for future research would be to account for different driving styles. In fact, several studies have shown that it is possible to distinguish amongst different driver categories (aggressive, mild, et cetera), but at present only one generic set of parameters is used.

The last direction which should be indicated is more broadly connected with the overall idea behind the OC concept. As remarked throughout the whole thesis, the format has been conceived to assist vehicles manufacturer in product development, from the early stage to sale phases. We have to some extent illustrated a possible application in the context of product selection, but a fundamental part of the process is entailed by the pure development phase. From this perspective, it is clear that the potential of the OC when it comes to optimisation purposes must still be tested. There are two macro-areas of research to explore. The first one concerns the possibility of using the OC format offline. The inspiration comes from mainly recent studies, for example the ones authored by Ghandriz (2018, 2020), Ghandriz, Hellgren, et al. (2016), and Ghandriz, Jacobson, Laine, et al. (2020). In most cases, only information about the road grade is included in the modelling of the environment, whilst it would be beneficial to exploit all the stochastic models developed so far. This would allow to optimise the vehicle's configuration considering all the relevant factors.

The second research opportunity resides in the possibility of using the OC description (or some methods and tools borrowed from it) for online estimation. The idea has only been formulated in embryonic form, but can be worthy of further investigations.

Bibliography

Amirjamshidi, Glareh and Matthew J. Roorda (2015). "Development of simulated driving cycles for light, medium, and heavy duty trucks: Case of the Toronto Waterfront Area". In: *Transportation Research Part D: Transport and Environment* 34, pp. 255–266. ISSN: 1361-9209. DOI: https://doi.org/10.1016/j.trd.2014.11.010.

Åsbogåard, M., L. Johannesson, D. Angervall, and P. Johansson (2007). "Improving system design of a hybrid powertrain using stochastic drive cycles and dynamic programming". In: ed. by SAE World Congress and Exhibition. Detroit, MI, USA.

Ashatari, A., E. Bibeau, and S. Shahidinejad (2014). "Using large driving record samples and a stochastic approach for real-world driving cycle construction: Winnipeg driving cycle". In: *Transportation Science* 48.2, pp. 170–183.

Basso, Rafael, Balázs Kulcsár, Bo Egardt, Peter Lindroth, and Ivan Sanchez-Diaz (2019). "Energy consumption estimation integrated into the Electric Vehicle Routing Problem". In: *Transportation Research Part D: Transport and Environment* 69, pp. 141–167. ISSN: 1361-9209. DOI: https://doi.org/10.1016/j.trd.2019.01.006.

Basso, Rafael, Balázs Kulcsár, and Ivan Sanchez-Diaz (2021). "Electric vehicle routing problem with machine learning for energy prediction". In: *Transportation Research Part B: Methodological* 145, pp. 24–55. ISSN: 0191-2615. DOI: https://doi.org/10.1016/j.trb.2020.12.007.

Beckers, C. J. J., I. J. M. Besselink, and H. Nijmeijer (2019). "Modeling of Energy Losses During Cornering for Electric City Buses". In: *2019 IEEE Intelligent Transportation Systems Conference (ITSC)*, pp. 4164–4169. DOI: 10.1109/ITSC.2019.8917232.

Beckers, C. J. J., I. J. M. Besselink, and H. Nijmeijer (2020). "Assessing the impact of cornering losses on the energy consumption of electric city buses". In: *Transportation Research Part D: Transport and Environment* 86, p. 102360. ISSN: 1361-9209. DOI: https://doi.org/10.1016/j.trd.2020.102360.

Box, G., G. Jenkins, G. Reinsel, G. Ljung, and G. Ljung (2015). *Time Series Analysis: Forecasting and Control*. 5th ed. John Wiley & Sons.

Brady, John and Margaret O'Mahony (2016). "Development of a driving cycle to evaluate the energy economy of electric vehicles in urban areas". In: *Applied Energy* 177, pp. 165–178. ISSN: 0306-2619. DOI: https://doi.org/10.1016/j.apenergy.2016.05.094.

C. C. C. Service (2019). *Record-breaking temperatures for june*. https://ucsusa.org/climate/science.

Cadenas, Erasmo, Wilfrido Rivera, Rafael Campos-Amezcual, and Cristopher Heard (2016). "Wind Speed Prediction Using a Univariate ARIMA Model and a Multivariate NARX Model". In: *Energies* 9.2. ISSN: 1996-1073. DOI: 10.3390/en9020109.

Callery, S. (2019). *Climate change: How do we know*. Tech. rep. Two independence square, Washington D.C., U.S.: United States.

Chin, Edwin H. (1977). "Modeling daily precipitation occurrence process with Markov Chain". In: *Water Resources Research* 13.6, pp. 949–956. DOI: https://doi.org/10.1029/WR013i006p00949. eprint: https://agupubs.onlinelibrary.wiley.com/doi/pdf/10.1029/WR013i006p00949.

Cook, John, Dana Nuccitelli, Sarah A Green, Mark Richardson, Bärbel Winkler, Rob Painting, Robert Way, Peter Jacobs, and Andrew Skuce (May 2013). "Quantifying the consensus on anthropogenic global warming in the scientific literature". In: *Environmental Research Letters* 8.2, p. 024024. DOI: 10.1088/1748-9326/8/2/024024.

Edlund, Stefan and Per-Olov Fryk (Oct. 2004). "The Right Truck for the Job with Global Truck Application Descriptions". In: *SAE Technical Paper*. SAE International. DOI: 10.4271/2004-01-2645.

Erdem, Ergin and Jing Shi (2011). "ARMA based approaches for forecasting the tuple of wind speed and direction". In: *Applied Energy* 88.4, pp. 1405–1414. ISSN: 0306-2619. DOI: https://doi.org/10.1016/j.apenergy.2010.10.031.

Eriksson, A. (1997). *Simulation based methods and tools for comparison of powertrain concepts*.

European Commission (2014a). *Regulation (eu) no 253/2014 of the european parliament and of the council of 26 february 2014 amending regulation (ec) no 510/2011 to define modalities for reaching the 2020 target to reduce co2 emissions from new light commercial vehicles*. https://eur-lex.europa.eu/legal-content/EN/TXT/?uri=OJ%3AL%3A2014%3A084%3ATOC.

European Commission (2014b). *Regulation (eu) no 333/2014 of the european parliament and of the council of 11 march 2014 amending regulation (ec) no 443/2009 to define modalities for reaching the 2020 target to reduce co2 emissions from new passenger cars*. https://eur-lex.europa.eu/legal-content/EN/TXT/?uri=OJ%3AL%3A2014%3A084%3ATOC.

European Commission (2017). *Commission regulation (eu) no 2017/2400. official journal of european union 60.l 247 (dec. 2017)*. https://eur-lex.europa.eu/legal-content/EN/TXT/?uri=OJ%3AL%3A2017%3A349%3ATOC.

European Commission (2019). *Vehicle Energy Consumption calculation Tool – VECTO*. https://ec.europa.eu/clima/policies/transport/vehicles/vecto_en.

European Environmental Agency (2019). *Greenhouse gas emissions from transport*. Tech. rep. European Environmental Agency.

Eurostat (2019). *Greenhouse gas emission statistics – emission inventories*. https://ec.europa.eu/eurostat/statistics-explained/index.php/Greenhouse_gas_emission_statistics.

Evans, Lawrence C. (2010). *Partial Differential Equations*. 2nd. American Mathematical Society.

Eymen, A. and Ü. Köylü (2019). "Seasonal trend analysis and ARIMA modeling of relative humidity and wind speed time series around Yamula Dam". In: *Meteorol Atmos Phys* 131, pp. 601–612. DOI: 10.1007/s00703-018-0591-8.

Fisher, N. I. (1993). *Statistical Analysis of Circular Data*. Cambridge University Press. DOI: 10.1017/CBO9780511564345.

Fontaras, G., M. Rexeis, P. Dilara, S. Hausberger, and K. Anagnostopoulos (2013). "he development of a simulation tool for monitoring heavy-duty vehicle co2 emissions and fuel consumption in europe". In: ed. by 11th International Conference on Engines and Vehicles.

G. C. Project (2017). *The global carbon atlas, co2 emissions*. http://www.globalcarbonatlas.org/en/CO2-emissions.

Gabriel, K. R. and J. Neumann (1962). "A Markov chain model for daily rainfall occurrence at Tel Aviv". In: *Quarterly Journal of the Royal Meteorological Society* 88.375, pp. 90–95. DOI: https://doi.org/10.1002/qj.49708837511. eprint: https://rmets.onlinelibrary.wiley.com/doi/pdf/10.1002/qj.49708837511.

Ghandriz, T. (2018). *Transportation Mission Based Optimization of Heavy Vehicle Fleets including Propulsion Tailoring*.

Ghandriz, T. (2020). "Transportation Mission-Based Optimization of Heavy Combination Road Vehicles and Distributed Propulsion, Including Predictive Energy and Motion Control". PhD thesis. Chalmers University of Technology. URL: https://research.chalmers.se/en/publication/520358.

Ghandriz, T., J. Hellgren, M. Islam, L. Laine, and B. Jacobson (2016). "Optimization based design of heterogeneous truck fleet and electric propulsion". In: ed. by IEEE 19th International Conference on Intelligent Transportation Systems (ITSC). Rio de Janeiro, pp. 328–335.

Ghandriz, T., B. Jacobson, L. Laine, and J. Hellgren (2020). "Impact of automated driving systems on road freight transport and electrified propulsion of heavy vehicles". In: *Transportation Research Part C: Emerging Technologies* 115.

Ghandriz, T., B. Jacobson, P. Nilsson, L. Laine, and N. Fröjd (2020). "Computationally Efficient Nonlinear One- and Two-Track Models for Multitrailer Road Vehicles". In: *IEEE Access* 8, pp. 203854–203875. DOI: 10.1109/ACCESS.2020.3037035.

Grimmett, G. and D. Stirzaker (2020). *Probability and random processes*. 4th ed. Oxford university press.

Guiggiani, M. (2018). *The Science of Vehicle Dynamics*. 2nd. Cham(Switzerland): Springer International.

Hausfather, Z. (2020). *State of the climate: 2020 set to be the first ot second warmest year on record*. https://www.carbonbrief.org/state-of-the-climate-2020-set-to-be-first-or-second-warmest-year-on-record.

Hocaoğlu, Fatih Onur, Ömer Nezih Gerek, and Mehmet Kurban (2010). "A novel wind speed modeling approach using atmospheric pressure observations and hidden Markov models". In: *Journal of Wind Engineering and Industrial Aerodynamics* 98.8, pp. 472–481. ISSN: 0167-6105. DOI: https://doi.org/10.1016/j.jweia.2010.02.003.

Husak, Gregory J., Joel Michaelsen, and Chris Funk (2007). "Use of the gamma distribution to represent monthly rainfall in Africa for drought monitoring applications". In: *International Journal of Climatology* 27.7, pp. 935–944. DOI: https://doi.org/10.1002/joc.1441. eprint: https://rmets.onlinelibrary.wiley.com/doi/pdf/10.1002/joc.1441.

Jacobson, B., S. Berglund, and P. Pettersson (n.d.). *Vehprop – a simulation model library*. http://www.chalmers.se/en/departments/m2/research/veas/Pages/VehProp.aspx.

Johannesson, P., K. Podgórski, and I. Rychlik (2016). "Modelling roughness of road profiles on parallel tracks using roughness indicators". In: *International Journal of Vehicle Design (IJVD)* 70.2. DOI: 1.

Johannesson, P., K. Podgórski, and I. Rychlik (2017). "Laplace distribution models for road topography and roughness". In: *International Journal of Vehicle Performance (IJVP)* 3.3.

Johannesson, P., K. Podgórski, I. Rychlik, and N. Shariati (2016). "AR(1) time series with autoregressive gamma variance for road topography modeling". In: *Probabilistic Engineering Mechanics* 34, pp. 106–116.

Kamble, Sanghpriya H., Tom V. Mathew, and G.K. Sharma (2009). "Development of real-world driving cycle: Case study of Pune, India". In: *Transportation Research Part D: Transport and Environment* 14.2, pp. 132–140. ISSN: 1361-9209. DOI: https://doi.org/10.1016/j.trd.2008.11.008.

Kessels, F. (2019). *Traffic flow modelling*. Springer. DOI: 10.1007/978-3-319-78695-7.

Kivekäs, K., J. Vepsäläinen, and K. Tammi (2018). "Stochastic Driving Cycle Synthesis for Analyzing the Energy Consumption of a Battery Electric Bus". In: *IEEE Access* 6, pp. 55586–55598. DOI: 10.1109/ACCESS.2018.2871574.

Kivekäs, K., J. Vepsäläinen, K. Tammi, and J. Anttila (2017). "Influence of Driving Cycle Uncertainty on Electric City Bus Energy Consumption". In: *2017 IEEE Vehicle Power and Propulsion Conference (VPPC)*, pp. 1–5. DOI: 10.1109/VPPC.2017.8331014.

Kobayashi, T., E. Katsuyama, H. Sugiura, Y. Hattori, E. Ono, and M. Yamamoto (2020). "Theoretical analysis of tyre slip power dissipation mechanism using brush model". In: *Vehicle System Dynamics* 58.8, pp. 1242–1256. DOI: 10.1080/00423114.2019.1612926. eprint: https://doi.org/10.1080/00423114.2019.1612926.

Kobayashi, T., E. Katsuyama, H. Sugiura, E. Ono, and M. Yamamoto (2017). "Direct yaw moment control and power consumption of in-wheel motor vehicle in steady-state turning". In: *Vehicle System Dynamics* 55.1, pp. 104–120. DOI: 10.1080/00423114.2016.1246737. eprint: https://doi.org/10.1080/00423114.2016.1246737.

Kobayashi, T., E. Katsuyama, H. Sugiura, E. Ono, and M. Yamamoto (2018). "Efficient direct yaw moment control: tyre slip power loss minimisation for four-independent wheel drive vehicle". In: *Vehicle System Dynamics* 56.5, pp. 719–733. DOI: 10.1080/00423114.2017.1330483. eprint: https://doi.org/10.1080/00423114.2017.1330483.

Kumar, V., Shanu, and Jahangeer (2017). "Statistical distribution of rainfall in Uttarakhand, India". In: *Appl Water Sci* 7, pp. 4765–4776. DOI: 10.1007/s13201-017-0586-5.

La Rocca, Paola, Daniele Riggi, and Francesco Riggi (Apr. 2010). "Time series analysis of barometric pressure data". In: *European Journal of Physics* 31.3, pp. 645–655. DOI: 10.1088/0143-0807/31/3/022.

Lee, T. K. and Z. S. Filipi (2011). "Synthesis of real-world driving cycles using stochastic process and statistical methodology". In: *International Journal of Vehicle Design* 57.1, pp. 17–36.

Lee, T., B. Adornato, and Z. S. Filipi (2011). "Synthesis of Real-World Driving Cycles and Their Use for Estimating PHEV Energy Consumption and Charging Opportunities: Case Study for Midwest/U.S." In: *IEEE Transactions on Vehicular Technology* 60.9, pp. 4153–4163. DOI: 10.1109/TVT.2011.2168251.

Lin, Jie and Debbie A Niemeier (2002). "An exploratory analysis comparing a stochastic driving cycle to California's regulatory cycle". In: *Atmospheric Environment* 36.38, pp. 5759–5770. ISSN: 1352-2310. DOI: https://doi.org/10.1016/S1352-2310(02)00695-7.

Liu, Y., M. C. Roberts, and R. Sioshansi (2018). "A vector autoregression weather model for electricity supply and demand modeling". In: *Journal of Modern Power Systems and Clean Energy* 6.4, pp. 763–776. DOI: 10.1007/s40565-017-0365-1.

Llopis-Castelló, David, Ana Maria Pérez-Zuriaga, Francisco Javier Camacho-Torregrosa, and Alfredo García (2018). "Impact of horizontal geometric design of two-lane rural roads on vehicle co2 emissions". In: *Transportation Research Part D: Transport and Environment* 59, pp. 46–57. ISSN: 1361-9209. DOI: https://doi.org/10.1016/j.trd.2017.12.020.

Lütkepohl, H. (2010). *New Introduction to Multiple Time Series Analysis*. Springer, Berlin, Heidelberg. DOI: https://doi.org/10.1007/978-3-540-27752-1.

Michon, John A. (1985). "A Critical View of Driver Behavior Models: What Do We Know, What Should We Do?" In: *Human Behavior and Traffic Safety*. Ed. by Leonard Evans and Richard C. Schwing. Boston, MA: Springer US, pp. 485–524. ISBN: 978-1-4613-2173-6. DOI: 10.1007/978-1-4613-2173-6_19.

Naghizadeh, M. (2003). "DEVELOPMENT OF CAR DRIVE CYCLE FOR SIMULATION OF EMISSIONS AND FUEL ECONOMY". In:

Nordström, E. (2020). "Advanced Modelling and Energy Efficiency Prediction for Road Vehicles". MA thesis. Umeå University.

Ntziachristos, L. and Z. Samaras (July 2018). *EMEP/EEA air pollutant emission inventory guidebook 2016 Part B.1.A.3.b.i-iv Road transport 2018*. Tech. rep. EEA Report No 21/2016. Copenhagen, Denmark: European Environment Agency: Chalmers University of Technology.

Nyberg, P. (2015). "Evaluation, generation and transformation of driving cycles". PhD thesis. Linköping, Sweden.

Ockendon, John R., Sam Howison, Andrew Lacey, and Alexander B. Movchan (2003). *Applied Partial Differential Equations*. Oxford University Press.

Pacejka, H. B. (2012). *Tyre and vehicle dynamics*. 3rd. Oxford, UK: Elsevier/Butterworth-Heinemann.

Pettersson, P. (2019). "Operating cycle representation for road vehicles". PhD thesis. Chalmers University of Technology.

Pettersson, P., S. Berglund, B. J. Jacobson, L. Fast, P. Johannesson, and F. Santandrea (2019). "A proposal for an operating cycle description format for road transport missions". In: *European Transport Research Review* 10.31, pp. 1–19.

Pettersson, P., B. Jacobson, and S. Berglund (2016). *A model of an automatically shifted truck for prediction of longitudinal performance on an operating cycle*. Tech. rep. Chalmers University of Technology.

Pettersson, P., P. Johannesson, B. Jacobson, F. Bruzelius, L. Fast, and S. Berglund (2019). "A statistical operating cycle description for prediction of road vehicles' energy consumption". In: *Transportation Research Part D: Transport and Environment* 73, pp. 205–229.

Romano, Luigi, Fredrik Bruzelius, and Bengt Jacobson (2020a). "Brush tyre models for large camber angles and steering speeds". In: *Vehicle System Dynamics* 0.0, pp. 1–52. DOI: 10.1080/00423114.2020.1854320. eprint: https://doi.org/10.1080/00423114.2020.1854320.

Romano, Luigi, Fredrik Bruzelius, and Bengt Jacobson (2020b). "Unsteady-state brush theory". In: *Vehicle System Dynamics* 0.0, pp. 1–29. DOI: 10.1080/00423114.2020.1774625. eprint: https://doi.org/10.1080/00423114.2020.1774625.

Romano, Luigi, Fredrik Bruzelius, and Bengt Jacobson (2021). "A Brush Tyre Model with Standstill Handler for Energy Efficiency Studies". In: *Commercial Vehicle Technology 2020/2021. Proceedings*. DOI: 10.1007/978-3-658-29717-6_10.

Sciarretta, A. (2020). *Energy-Efficient Driving of Road Vehicles*. Springer (Cham), Springer Nature Switzerland AG.

Sentoff, K., L. Aultman-Hall, and B. Holmé (2015). "Implications of driving style on road grade for accurate vehicle data and emissions estimates". In: *Transportation Research Part D: Transport and Environment* 35, pp. 175–188.

Silvas, E. (Nov. 2015). "Integrated optimal design for hybrid electric vehicles". English. Proefschrift. PhD thesis. Department of Mechanical Engineering. ISBN: 978-90-386-3968-0.

Silvas, E., K. Hereijgers, H. Peng, T. Hofman, and M. Steinbuch (2016). "Synthesis of Realistic Driving Cycles With High Accuracy and Computational Speed, Including Slope Information". In: *IEEE Transactions on Vehicular Technology* 65.6, pp. 4118–4128. DOI: 10.1109/TVT.2016.2546338.

Tazelaar, Edwin, Jogchum Bruinsma, Bram Veenhuizen, and Paul Van den Bosch (2009). "Driving cycle characterization and generation, for design and control of fuel cell buses". In: *World Electric Vehicle Journal* 3.4, pp. 812–819. DOI: 10.3390/wevj3040812.

Tennekes, H. (1973). "The Logarithmic Wind Profile". In: *Journal of Atmospheric Sciences* 30.2, pp. 234–238. DOI: 10.1175/1520-0469(1973)030<0234:TLWP>2.0.CO;2.

Tol, Richard S.J. (2014). "Quantifying the consensus on anthropogenic global warming in the literature: A re-analysis". In: *Energy Policy* 73, pp. 701–705. ISSN: 0301-4215. DOI: https://doi.org/10.1016/j.enpol.2014.04.045.

Torinsson, J., M. Jonasson, D. Yang, and B. Jacobson (2020). "Energy reduction by power loss minimisation through wheel torque allocation in electric vehicles: a simulation-based approach". In: *Vehicle System Dynamics* 0.0, pp. 1–24. DOI: 10.1080/00423114.2020.1858121. eprint: https://doi.org/10.1080/00423114.2020.1858121.

U. S. E. P. Agency (2019). *Overview of greenhouse gases*. Tech. rep. Two independence square, Washington D.C., U.S.: United States: Environmental Protection Agency.

Union of concerned scientists (2019). *Global warming*. Tech. rep. Cambridge, MA, U.S.

Wyatt, D. W., H. Li., and J. E. Tate (2014). "The impact of road grade on carbon dioxide (co2) emissions of passenger vehicle in real-world driving". In: *Transportation Research Part D: Transport and Environment* 32, pp. 160–170.

Zou, Zhanjiang, Scott Davis, Kevin Beaty, Michael O'Keefe, Terry Hendricks, Robert Rehn, Steve Weissner, and V. K. Sharma (Mar. 2004). "A New Composite Drive Cycle for Heavy-Duty Hybrid Electric Class 4-6 Vehicles". In: *SAE Technical Paper*. SAE International. DOI: 10.4271/2004-01-1052.

Appendix A

Stochastic processes

The aim of this appendix is to give a more formal introduction to the notation and the main mathematical tools used in the building of the sOC. In particular, in the derivation of the models illustrated in Chapter 2, a pivotal role is played by some simple stochastic processes. There are three main classes of stochastic processes used in this thesis: *autoregressive processes*, *Markov processes* and *Poisson processes*.

The two main references for the notation and the theory introduced here are Box et al. (2015), Grimmett and Stirzaker (2020), and Lütkepohl (2010).

A.1 Autoregressive processes

A time series can be seen as a sequence of random variables, i.e. a family $\{X_k : k \in K\}$ indexed by some set K, where each X_k is a random variable which takes value in a set called *state space* and denoted with $\mathcal{S}_X$. In this thesis, we will consistently use the short notation $\{X_k\} = \{X_k\}_{k=0}^N = \{X_0, X_1, \dots, X_N\}$.

Linear models constitute a class of particularly relevant stochastic processes, which are relatively easy to study and parametrise. These assume that time series are generated by linear aggregation of random innovations (Box et al. 2015). Parsimonious representations can be achieved with relatively low effort by employing autoregressive-moving average (ARMA) terms.

Intuitively, a stationary process $\{X_k\}$ is a process whose statistical properties do not vary over the time, or, more precisely, are unaffected by a change of time origin. This property can be formalised mathematically as follows.

Definition A.1.1. *A stochastic process is said to be stationary if the joint probability distribution associated with m observations $X_{k_1} = x_{k_1}, X_{k_2} = x_{k_2}, \dots, X_{k_m} = x_{k_m}$ at any set of times $t_1, t_2, \dots, t_m$ is the same as the associated with m observations $X_{k_{1+h}} = x_{k_{1+h}}, X_{k_{2+h}} = x_{k_{2+h}}, \dots, X_{k_{m+h}} = x_{k_{m+h}}$ made at times $t_1 + h, t_2 + h, \dots, t_m + h$.*

Moreover, for $m = 1$, the stationarity property A.1.1 also implies that the process *mean* and *variance* μ and σ_X^2, given respectively by

$$\mu = \mathbb{E}(X_k), \tag{A.1a}$$

$$\sigma_X^2 = \mathbb{E}\Big[(X_k - \mu)^2\Big]. \tag{A.1b}$$

are the same for all $k \in K$. A very special class of stochastic processes is the one of *normal* or *Gaussian processes*, i.e. stochastic processes whose probability distributions are multivariate normal or Gaussian distributions for any set of times. It can be demonstrated that such processes are always stationary. We will introduce in details three types of stationary models whose practical relevance is well documented in literature. These are, in order: *autoregressive models*, *moving-average*, and *autoregressive moving-average*.

A.1.1 Autoregressive models

One of the simplest stochastic processes used to practically represent a timeseries is an *autoregressive model*. In this model, the current value of the process is expressed as a linear combination of p previous states, plus an innovation term e_k which follows a known distribution[1]. In short notation, an autoregressve process of order p is therefore referred to as AR(p). Denoting the value of a process at equally spaced times k, $k-1$, k_2, ... by X_k, X_{k-1}, X_{k-2}, ..., then we have in formulae

$$X_k = c + \phi_1 X_{k-1} + \phi_2 X_{k-2} + \cdots + \phi_p X_{k-p} + e_k. \tag{A.2}$$

The above Eq. (A.2) can restated more succinctly after defining the *lag operator* L such that $L^i X_k = X_{k-i}$ ad the degree p AR *lag operator polynomial* $\phi(L)$:

$$\phi(L) = 1 - \phi_1 L - \phi_2 L^2 - \cdots - \phi_p L^p. \tag{A.3}$$

Combining Eqs. (A.2) and (A.3) yields

$$\phi(L) X_k = c + e_k. \tag{A.4}$$

For a Gaussian AR(p) model, i.e. with $e_k \sim \mathcal{N}(0, \sigma_e^2)$, an alternative representation of Eq.(A.4) is given by

$$X_k = \mu + \psi(L) e_k, \tag{A.5}$$

where μ is the unconditional mean of the process reading

$$\mu = \phi(L)^{-1} c = \mathbb{E}\Big[\phi(L)^{-1}(c + e_k)\Big], \tag{A.6}$$

and $\psi(L) = \phi(L)^{-1}$ is a rational, infinite-degree lag operator. For a generic AR(p), on the other hand, the computation of the variance is more involving and requires the knowledge of the theoretical autocorrelations. The reader is referred to e.g. Box et al. (ibid.) for a detailed discussion. The analytical expression for the process variance considerably simplifies for the case of an AR(1) model, yielding

$$\sigma_X^2 = \frac{\sigma_e^2}{1 - \phi_1^2}. \tag{A.7}$$

[1] Throughout this thesis, we will implicitly assume that the innovation term is normally distributed with zero mean, i.e. $e_k \sim \mathcal{N}(0, \sigma_e^2)$. This requirement, together with opportune restrictions on the values assumed by the coefficients ϕ_i in Eq. (A.2), ensures the model to be stationary. The only model treated in this thesis which does not satisfy the above criteria is the stationary Laplace model used for the road roughness used in Chapter 2 and developed by Johannesson, Podgórski, and Rychlik (2016). This, however, will not be discussed in detail.

The relationship between the innovation and process variances σ_e^2 and σ_X^2, respectively, is of particular interest when it comes to the estimation and interpretation of the statistical properties of a model, since σ_X^2 may happen to be more easily inferred from actual data. A Gaussian AR(p) model is fully characterised by $p+2$ parameters, for example $\mu, \phi_1, \phi_2, \dots \phi_q$ and σ_e^2[2].

A.1.2 Moving average models

The *moving average* model also plays a fundamental role in the representation of stochastic timeseries. It assumes that the current observation X_k depends linearly on a combination of q previous innovations. A moving average process is thus abbreviated as MA(q) and described mathematically as follows:

$$X_k = c + e_k + \theta_1 e_{k-1} + \theta_2 e_{k-2} + \cdots + \theta_q e_{k-q}. \tag{A.8}$$

Defining the *moving average operator* of order q by

$$\theta(L) = 1 + \theta_1 L + \theta_2 L^2 + \cdots + \theta_q L^q, \tag{A.9}$$

we can recast Eq. (A.8) more conveniently as

$$X_k = c + \theta(L) e_k. \tag{A.10}$$

It becomes quite obvious from Eq. (A.10) that for a MA(q) model the process mean is given simply by $\mu = c$ independently of the order q. In this case, the model is fully parametrised by the $q+2$ coefficients $\mu, \theta_1, \theta_2, \dots, \theta_q$ and σ_e^2.

A.1.3 Autoregressive moving average model

This model is obtained by combining an autoregressive AR(p) model with a moving-average MA(q). Therefore, it immediately follows that

$$X_k = c + \phi_1 X_{k-1} + \cdots + \phi_p X_{k-p} + e_k + \theta_1 e_{k-1} + \cdots + \theta_q e_{k-q}, \tag{A.11}$$

or equivalently

$$\phi(L) X_k = c + \theta(L) e_k. \tag{A.12}$$

Remark A.1.1. *An alternative representation of an ARMA(p, q) model is given by*

$$X_k = \mu + \psi(L) e_k, \tag{A.13}$$

where μ is the unconditional mean of the process reading

$$\mu = \phi(L)^{-1} c, \tag{A.14}$$

and $\psi(L) = \phi(L)^{-1}\theta(L)$ is a rational, infinite-degree lag operator.

[2]The choice is not unique, since another possible parametrisation consists in using c in place of μ.

A.1.4 Vector autoregressive processes

The notions of autoregressive model AR(p), moving-average MA(q) and mixed autoregressive moving-average ARMA(p, q) can be extended to a vector-valued stochastic process $\{\boldsymbol{X}_k\}$ (Lütkepohl 2010), called VARMA(p, q). In this case, the equivalent notation using the lag operator is

$$\boldsymbol{\Phi}(L)\boldsymbol{X}_k = \boldsymbol{c} + \boldsymbol{\Theta}(L)\boldsymbol{e}_k, \tag{A.15}$$

where $\boldsymbol{c} \in \mathbb{R}^n$ is a constant offset and

$$\boldsymbol{\Phi}(L) = \mathbf{I} - \sum_{j=1}^{p} \boldsymbol{\Phi}_j L^j, \tag{A.16a}$$

$$\boldsymbol{\Theta}(L) = \mathbf{I} + \sum_{i=1}^{q} \boldsymbol{\Theta}_i L^i. \tag{A.16b}$$

In Eqs. (A.16a) and (A.16b), respectively, each $\boldsymbol{\Phi}_j \in \mathbb{R}^{n\times n}$ is a matrix of AR coefficients, and each $\boldsymbol{\Theta}_i \in \mathbb{R}^{n\times n}$ is a matrix of MA coefficients. A VARMA(p, q) model is fully characterised by $2n + n^2(p + q)$ parameters.

A.1.5 Nonstationary models

Many real processes encountered in nature do not vary around a fixed mean. Such behaviour can be captured eventually using a nonstationary model. Autoregressive models describing nonstationary timeseries are also called *autoregressive integrated moving average processes* and abbreviated ARIMA(p, d, q). In formulae, we have

$$\phi(L)(1 - L)^d X_k = c + \theta(L)e_k, \tag{A.17}$$

where, as usual, $\phi(L)$ and $\theta(L)$ are stable autoregressive and moving average operators. Defining $(1 - L)^d X_k \triangleq W_k$, Eq.(A.17) can be restated as

$$\phi(L)W_k = c + \theta(L)e_k. \tag{A.18}$$

It is seen from Eq. (A.18) that a nonstationary autoregressive process can be interpreted as a stationary one when considering the difference up to the d_{th} order.

A.2 Markov processes

Markov processes can be either discrete or continuous in time. We will only review the discrete version, since it is the one used in the building of the models of Chapter 2. In this context, a Markov processes describes sequences of events in which the probability of each event only depends on the state attained in the previous event. This property, called *Markov property*, is formalised mathematically below.

Definition A.2.1. *Let $\{X_k\}$ be a discrete stochastic process which takes its values in a state space $\mathcal{S}_X = \{x_1, x_2, \ldots, x_n\}$ and let $x_i \in \mathcal{S}_X$. If*

$$\mathbb{P}\Big(X_{k+1} = x_{i_{k+1}} \;\Big|\; X_1 = x_{i_1}, X_2 = x_{i_2}, \ldots, X_k = x_{i_k}\Big) = \mathbb{P}\Big(X_{k+1} = x_{i_{k+1}} \;\Big|\; X_k = x_{i_k}\Big), \tag{A.19}$$

then $\{X_k\}$ is called a discrete Markov process.

In the following definition we introduce the notation for the probability p_{ij} of taking a step from the current state x_i to the next state x_j.

Definition A.2.2. *Consider a Markov process as in Def. A.2.1. The probability p_{ij} of taking a step from current state $x_i \in \mathcal{S}_X$ to a next state $x_j \in \mathcal{S}_X$ is given by*

$$p_{ij} = \mathbb{P}\Big(X_{k+1} = x_j \;\Big|\; X_k = x_i\Big). \tag{A.20}$$

The transition probabilities p_{ij}, $\forall x_i, x_j \in \mathcal{S}_X$, are collected in the transition probability matrix, or Markov matrix, denoted here with $\mathbf{P} \in \mathbb{R}^{n\times n}$, where n is the number of states. The entries of the Markov matrix are all non-negative, i.e. $p_{ij} \geq 0$, and satisfy the following property.

Property A.2.1. *Consider a Markov process as in Def. A.2.1. Then, every entry p_{ij} of the Markov matrix $\mathbf{P}$ satisfies:*

$$\sum_j p_{ij} = \sum_j \mathbb{P}\Big(X_{k+1} = x_j \;\Big|\; X_k = x_i\Big) = 1. \tag{A.21}$$

The Markov properties listed above can be extended to cover a more general class of processes. For example, two and three-dimensional Markov processes are discussed extensively in Silvas (2015).

A.3 Marked Poisson processes

Another stochastic process which may be useful to introduce is the marked Poisson. We will give a quick illustration of a Poisson process assuming the time t as independent variable, but the discussion can be extended immediately if we think instead of a generic position x. With the premises above, a Poisson process $N(t)$ with intensity λ can be interpreted as the number of events observed up to time t, given that the inter-arrival times are independent exponentials with parameter λ. In formulae:

$$\mathbb{P}(N(t) = k) = \mathcal{P}_\lambda(t) = \frac{(\lambda t)^k}{k!}\mathrm{e}^{-\lambda t}, \qquad k \geq 0, \tag{A.22}$$

where we have denoted with $\mathcal{P}_\lambda(t)$ the Poisson distribution with parameter λ. Since exponential holding times are memory-less, we also deduce that a Poisson process satisfies the Markov property A.2.1 in the continuous time setting.

An interesting relationship holds between the Poisson distribution $\mathcal{P}_\lambda(\cdot)$ and the exponential one. In fact, whist the Poisson distribution provides a description of the number of occurrences per interval of time, the exponential provides a description of the length of time between two subsequent occurrences. This can be understood by considering that, if an event occurs on average at the rate of λ per unit of time, then there will be on average λt occurrences during an interval of length t. Indeed, the probability that an event occurs during t units of time is given by

$$\mathbb{P}(T \leq t) = 1 - \mathbb{P}(N(t) = 0) = 1 - \mathrm{e}^{-\lambda t}, \tag{A.23}$$

which is the CDF of the exponential distribution $\mathcal{E}(\lambda) = \mathrm{e}^{-\lambda t}$. A marked Poisson process $\{X_k, Y_k\}$ is composed of a point process with associated mark(s). It be interpreted as a sequence of random variables $\{(X_k, Y_k) : k \in K\}$ indexed by some set K, where both X_k and Y_k are random variables taking values in their respective state spaces, denoted with $\mathcal{S}_X$ and $\mathcal{S}_Y$, respectively. We can think of X_k as a location either in time or space, and to Y_k as a *mark*.

Appendix B

Probability distributions

Some useful distributions used in the building of the OC format are reported here for convenience.

Uniform distribution

A uniform distribution with parameters $-\infty < a < b < \infty$ is denoted with $\mathcal{U}(a, b)$. The PDF of a uniform distribution is given by

$$f(x; a, b) = \begin{cases} \dfrac{1}{b-a}, & a \leq x \leq b, \\ 0, & x < a,\ x > b. \end{cases} \tag{B.1}$$

Normal distribution

A normal distribution with mean $\mu \in \mathbb{R}$ and variance $\sigma^2 > 0$ is denoted with $\mathcal{N}(\mu, \sigma^2)$ and its PDF is given by

$$f(x; \mu, \sigma) = \frac{1}{\sigma\sqrt{2\pi}} \mathrm{e}^{-\frac{1}{2}\left(\frac{x-\mu}{\sigma}\right)^2}, \qquad x \in \mathbb{R}. \tag{B.2}$$

Exponential distribution

An exponential distribution with parameter $\lambda > 0$ is denoted with $\mathcal{E}(\lambda)$ and its PDF is given by

$$f(x; \lambda) = \begin{cases} \lambda \mathrm{e}^{-\lambda x}, & x \geq 0, \\ 0, & x < 0. \end{cases} \tag{B.3}$$

Poisson distribution

A Poisson distribution with parameter $0 < \lambda < \infty$ is denoted with $\mathcal{P}(\lambda)$ and its PMF is given by

$$f(k; \lambda) = \mathbb{P}(X(t) = k) = \frac{(\lambda t)^k \mathrm{e}^{-\lambda t}}{k!}, \qquad k \in \mathbb{N}_0. \tag{B.4}$$

Gamma distribution

A gamma distribution with shape and rate parameters $\alpha, \beta > 0$, respectively, is denoted by $\mathrm{Ga}(\alpha, \beta)$ and its PDF is given by

$$f(x; \alpha, \beta) = \frac{\beta^\alpha}{\Gamma(\alpha)} x^{\alpha-1} \mathrm{e}^{-\beta x}, \qquad x > 0, \tag{B.5}$$

where the gamma function $\Gamma(\cdot)$ is defined as

$$\Gamma(z) = \int_0^\infty x^{z-1} \mathrm{e}^{-x} \, \mathrm{d}x, \qquad \mathrm{Re}(z) > 0. \tag{B.6}$$

Part II

Appended papers

Paper 1

A case study of usage modelling of heavy vehicles using the operating cycle description

Luigi Romano, Erik Nordström, Fredrik Bruzelius, Rickard Andersson and Bengt Jacobson

Submitted for journal publication.

The paper was reformatted for uniformity, but otherwise is unchanged.

Paper 1. A case study of usage modelling of heavy vehicles using the operating cycle description

Luigi Romano, Erik Nordström, Fredrik Bruzelius, Rickard Andersson and Bengt Jacobson

Paper 2

An enhanced stochastic operating cycle description including weather and traffic models

Luigi Romano, Pär Johannesson, Fredrik Bruzelius and Bengt Jacobson

Accepted for publication by Transportation Research Part D: Transport and Environment.

The paper was reformatted for uniformity, but otherwise is unchanged.

Paper 2. An enhanced stochastic operating cycle description including weather and traffic models

Luigi Romano, Pär Johannesson, Fredrik Bruzelius and Bengt Jacobson

Paper 3

A theoretical investigation on transient tyre slip losses using the brush theory

Luigi Romano, Francesco Timpone, Fredrik Bruzelius and Bengt Jacobson

Submitted for journal publication.

The paper was reformatted for uniformity, but otherwise is unchanged.

Paper 3. A theoretical investigation on transient tyre slip losses using the brush theory

Luigi Romano, Francesco Timpone, Fredrik Bruzelius and Bengt Jacobson